

REVISITING SPARSE MATRIX COLORING AND BICOLORING

ALEXIS MONTOISON*, GUILLAUME DALLE†, AND ASSEFAW GEBREMEDHIN‡

Abstract. Sparse matrix coloring and bicoloring are fundamental building blocks of sparse automatic differentiation. Bicoloring is particularly advantageous for rectangular Jacobian matrices with at least one dense row and column. Indeed, in such cases, unidirectional row or column coloring demands a number of colors equal to the number of rows or columns. We introduce a new strategy for bicoloring that encompasses both direct and substitution-based decomposition approaches. Our method reformulates the two variants of bicoloring as star and acyclic colorings of an augmented symmetric matrix. We extend the concept of neutral colors, previously exclusive to bicoloring, to symmetric colorings, and we propose a post-processing routine that neutralizes colors to further reduce the overall color count. We also present the Julia package `SparseMatrixColorings.jl`, which includes these new bicoloring algorithms alongside all standard coloring methods for sparse derivative matrix computation. Compared to `ColPack`, the Julia package also offers enhanced implementations for star and acyclic coloring, vertex ordering, as well as decomposition.

Key words. graph coloring, bicoloring, post-processing, sparsity patterns, Jacobian, Hessian, automatic differentiation, Julia

AMS subject classifications. 05C15, 65F50, 65D25, 68R10, 90C06

1. Introduction.

1.1. Context and motivation. Modern scientific computing makes heavy use of automatic differentiation (AD) to obtain derivatives of computer programs [6]. Such derivatives are relevant in a wide variety of settings, from differential equations and nonlinear optimization to machine learning. Whenever the objects of interest are sparse matrices (Jacobians or Hessians), their computation can be accelerated significantly [26]. However, reaping the benefits of sparsity comes with increased algorithmic and implementation challenges.

Consider a function $f : \mathbb{R}^n \rightarrow \mathbb{R}^m$ and its Jacobian matrix $J = \partial f(x)$ at a point x . For roughly the same cost as the evaluation of f , forward-mode AD evaluates a single Jacobian-vector product $u \mapsto Ju$, while reverse-mode AD evaluates a single Vector-Jacobian product $v \mapsto v^\top J$. Importantly, this is obtained without ever materializing the matrix J . Taking the seed $u = e_j$ (resp. $v = e_i$) to be a basis vector of the input space (resp. output space) lets us recover the j -th column (resp. i -th row) of the Jacobian. One can then iterate through basis vectors and reconstruct the full Jacobian, either column-wise or row-wise. The complexity of this recovery, expressed in number of calls to f , scales either with the input dimension n or with the output dimension m .

Luckily, when the Jacobian is sparse, focusing on the non-zero entries often speeds things up. For instance, if the non-zeros in columns j_1 and j_2 never overlap at any row, they can be recovered together in a single product $J(e_{j_1} + e_{j_2})$ without the non-zero entries getting mixed up. Making this insight actionable requires solving a *matrix coloring problem* [20], which determines the sets of columns or rows of J that can be evaluated simultaneously. The number of distinct colors obtained corresponds to the number of seeds required to recover all non-zero entries of J . The recovery complexity then scales with the number of colors c , rather than n or m .

*Argonne National Laboratory, IL, USA. E-mail: amontoison@anl.gov

†LVMET, ENPC, Institut Polytechnique de Paris, Univ Gustave Eiffel, Marne-la-Vallée, France. E-mail: guillaume.dalle@enpc.fr

‡Washington State University, School of EECS, WA, USA. E-mail: assefaw.gebremedhin@wsu.edu

Version of May 26, 2025.

In some cases, like for banded matrices, non-overlapping columns and rows are easy to find, and the number of colors remains much lower than the dimension (scaling with the number of bands). But when a few columns or rows exhibit dense structures, the number of colors required can increase significantly. This justifies a shift from unidirectional to bidirectional coloring, or *bicoloring* [11, 30], which handles columns and rows jointly by combining reverse-mode and forward-mode AD. We illustrate this idea on a rectangle matrix in Figure 1.1, where a dense row and a dense column impose a significant burden on any one-sided coloring scheme. As seen in Figure 1.2,



Fig. 1.1: Row coloring (left) and column coloring (right) of a rectangle matrix, requiring the same number of colors as the matrix dimensions (respectively 6 and 12 in this case).

bicoloring offers a solution to this problem by assigning colors to a subset of both columns and rows: colored columns to be computed in forward mode and colored rows to be computed in reverse mode.



Fig. 1.2: Bicoloring of a rectangle matrix, requiring only 2 colors for the rows (left) and 2 colors for the columns (right). In the central figure, each nonzero coefficient is colored using its row's color and its column's color, when it is not neutral.

1.2. Applications. In certain optimization problems, the structure of the Jacobian can make unidirectional coloring inefficient. This subsection highlights cases where bidirectional coloring leads to substantial improvements in the computation of Jacobians.

1.2.1. Nonlinear least-squares problems. In the Gauss-Newton method [5] for solving $\min_{x \in \mathbb{R}^n} \frac{1}{2} \|F(x)\|^2$, with $F : \mathbb{R}^n \rightarrow \mathbb{R}^m$, one must solve a sequence of linear least-squares subproblems. At iteration k , the subproblem is

$$\min_{d \in \mathbb{R}^n} \frac{1}{2} \|J(x_k)d + F(x_k)\|^2,$$

where $J(x) \in \mathbb{R}^{m \times n}$ is the Jacobian of F at x . When $m \gg n$, column coloring with forward-mode AD is typically used for efficient Jacobian computation. However, the presence of a dense row, due to a residual involving all variables (such as normalization constraints or global coupling terms) renders column coloring inefficient, as the entire row must be recovered regardless of compression. While row coloring with reverse-mode AD is an alternative, it tends to be inefficient when m is much larger than n (due to a large number of row colors). Bicoloring can improve performance by recovering sparse columns using forward-mode AD and a few dense rows using reverse-mode AD.

1.2.2. Equality-constrained optimization problems. For optimization problems of the form

$$\min_{x \in \mathbb{R}^n} \phi(x) \quad \text{subject to} \quad c(x) = 0,$$

where $\phi : \mathbb{R}^n \rightarrow \mathbb{R}$ and $c : \mathbb{R}^n \rightarrow \mathbb{R}^m$, the Jacobian $J(x) \in \mathbb{R}^{m \times n}$ of the constraints c is essential for forming the sequence of linear systems encountered in Newton-based interior-point methods [45]. In particular, the linear system at iteration k is given by the Karush–Kuhn–Tucker conditions:

$$\begin{bmatrix} \nabla_{xx}^2 \mathcal{L}(x_k, y_k) & J(x_k)^\top \\ J(x_k) & 0 \end{bmatrix} \begin{bmatrix} \Delta x \\ \Delta y \end{bmatrix} = - \begin{bmatrix} \nabla_x \mathcal{L}(x_k, y_k) \\ c(x_k) \end{bmatrix},$$

where $\mathcal{L}(x, y) = \phi(x) - y^\top c(x)$ and $y \in \mathbb{R}^m$ is a vector of Lagrange multipliers. When $m \ll n$, reverse-mode AD is typically more efficient for computing $J(x)$ because it propagates derivatives from a small number of outputs. Consequently, using a row coloring strategy is appropriate in this setting to maximize the benefits of reverse-mode AD. However, if a dense column appears in the Jacobian, due to multiple constraints depending on a common variable, a pure row coloring strategy becomes inefficient. Although column coloring using forward-mode AD is an alternative, bicoloring can improve performance by recovering dense columns using forward-mode AD and sparse rows using reverse-mode AD.

1.2.3. Optimal control problems. Discretized optimal control problems [3] often yield Jacobians with structured sparsity patterns, including both dense rows and columns. Consider the following optimal control problem:

$$\min_{x(\cdot), u(\cdot), p} C(x(\cdot), u(\cdot), p) \quad \text{subject to} \quad \begin{cases} \dot{x}(t) = f(x(t), u(t), p), & t \in [0, 1], \\ \int_0^1 g(x(t), u(t), p) dt = 0. \end{cases}$$

where C is a cost function, $x(t)$ is the state, $u(t)$ is the control, and p represents the parameters that influence the dynamics. In this formulation, p is also treated as a decision variable and optimized jointly with the state and control trajectories; this is particularly useful when p includes physical parameters or the final time t_f (after an appropriate time rescaling). Discretizing the interval $t = [0, 1]$ using a grid t_0, t_1, \dots, t_N with step sizes $h_i = t_{i+1} - t_i$, we define the discrete variables $X = (x_0, \dots, x_N)$ and $U = (u_0, \dots, u_N)$, where $x_i \approx x(t_i)$ and $u_i \approx u(t_i)$. Using a Crank–Nicolson (trapezoidal) scheme for the dynamics, we obtain for $i = 0, \dots, N-1$: $x_{i+1} - x_i - \frac{h_i}{2} (f(x_i, u_i, p) + f(x_{i+1}, u_{i+1}, p)) = 0$. Since p appears in every dynamic equation, its derivative contributes to every row of the Jacobian, resulting in a dense column. Similarly, discretizing the integral constraint via the trapezoidal rule gives: $\sum_{i=0}^{N-1} \frac{h_i}{2} (g(x_i, u_i, p) + g(x_{i+1}, u_{i+1}, p)) = 0$. This equation aggregates information over the entire time horizon, so its derivative with respect to all decision variables produces a dense row in the Jacobian. Note that this behavior is independent of the discretization scheme. Although the Crank–Nicolson scheme is easiest to describe, other schemes exhibit the same behavior.

A common strategy to mitigate these dense structures is to augment the state. For instance, instead of treating p as an explicit optimization variable, one can introduce an additional state variable $q(t)$ governed by $\dot{q}(t) = 0$, with $q(0) = p$. Likewise, the integral constraint can be reformulated by introducing an extra state $y(t)$ governed by

$\dot{y}(t) = g(x(t), u(t), p)$. Instead of adding new variables and constraints through these reformulations, bicoloring enables efficient Jacobian computation without increasing the problem size.

1.3. Related works. The first approaches for efficient computation of sparse Jacobians and Hessians were proposed by [Curtis et al. \[14\]](#) and [Powell and Toint \[41\]](#), respectively. Their connection to graph coloring was discovered by [Coleman and Moré \[9\]](#), [Coleman and Moré \[10\]](#), and [McCormick \[38\]](#), triggering an ambitious research effort to design coloring algorithms and related software [\[13\]](#). Because the relevant graph coloring problems are NP-hard, most of these algorithms are heuristic in nature. For a detailed account of related literature, see the survey by [Gebremedhin et al. \[20\]](#) and references therein. There are alternative methods for sparse AD which do not rely on colorings [\[26, Chapter 7\]](#), but we will not discuss them here.

Given a matrix $A \in \mathbb{R}^{m \times n}$ to compress, one seeks the smallest matrix of seeds $U \in \{0, 1\}^{n \times c}$ (resp. $V \in \{0, 1\}^{m \times c}$) such that the compressed matrix $B = AU$ (resp. $B = V^\top A$) contains all the information needed to recover A . In what follows, this recovery process is also called *decompression*. For *direct* decomposition, the non-zero entries of A should be directly readable in the compressed matrix B . For decomposition by *substitution*, the non-zero entries should be retrievable by solving a triangular system of equations. Choosing the right seeds is equivalent to assigning colors to columns or rows, and then partitioning basis vectors by color. This coloring interpretation requires encoding the matrix A as a graph: two popular representations are the bipartite graph \mathcal{G}_b linking rows to columns (for general matrices) and the adjacency graph \mathcal{G}_a linking columns with each other (for symmetric matrices). The requirement for injective decomposition define the families of colorings that can be used on these graphs (usually more restrictive than the standard distance-1 coloring). [Table 1.1](#) summarizes the coloring models used in derivative computation via direct and substitution-based methods. In all cases, the lower the number of distinct colors, the more efficient the compression.

	Direct method	Substitution method
Jacobian, unidirectional	<i>Distance-2 coloring</i>	NA
Hessian, unidirectional	<i>Star coloring</i>	<i>Acyclic coloring</i>
Jacobian, bidirectional	<i>Star bicoloring</i>	<i>Acyclic bicoloring</i>

Table 1.1: Overview of coloring problems in derivative computation via direct and substitution methods.

Central to our work are the studies focused on symmetric matrices (like Hessians). They give rise to specialized coloring variants: the *star coloring* and *acyclic coloring*, introduced by [Coleman and Moré \[10\]](#) and [Coleman and Cai \[8\]](#) under slightly different names. We use the terminology of [Gebremedhin et al. \[20\]](#), which underlines the importance of *two-colored substructures* in star and acyclic colorings of the adjacency graph \mathcal{G}_a . In a star coloring (which corresponds to direct decomposition), given any pair of colors, the induced subgraph is a *collection of stars*. In an acyclic coloring (which corresponds to decomposition by substitution), it is a *collection of trees*. These insights were exploited by [Gebremedhin et al. \[21, 22\]](#) to design efficient coloring and decomposition routines. [Figure 1.3a](#) showcases examples of star and acyclic colorings.

A coloring model of particular interest to us is bicoloring, which is used in computations of Jacobians and was suggested independently by [Hossain and Steihaug \[30\]](#) and [Coleman and Verma \[11\]](#). The core idea is that combining row and column

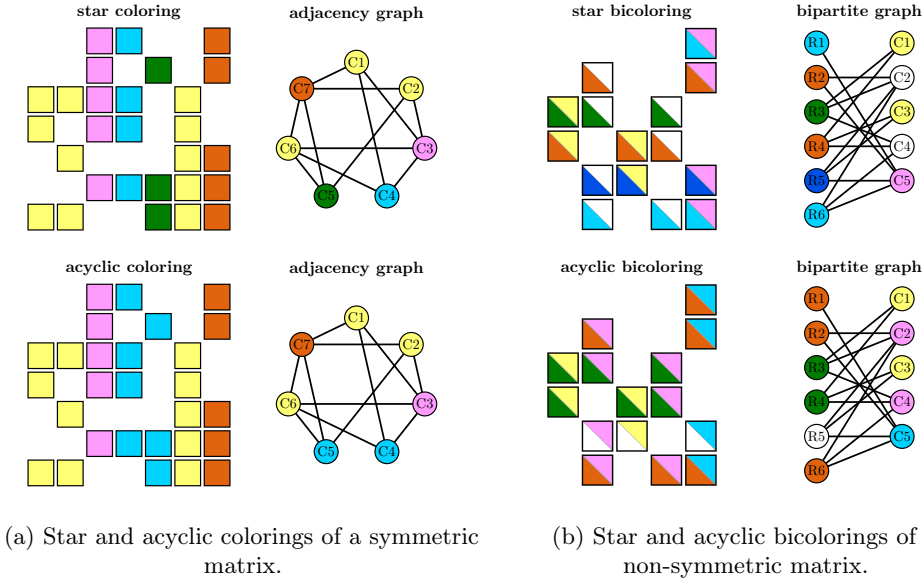


Fig. 1.3: Example colorings and bicolorings with their graph representations.

compression can yield fewer colors overall than either one separately. In this setting, recovery is based on a pair ($B_c = AU$, $B_r = V^T A$) of column- and row-compressed matrices rather than a single compressed matrix. The typical objective is to minimize the total number of seeds in (U, V) . Bicoloring may leave some columns (resp. rows) uncolored if all their non-zeros can already be recovered from the corresponding rows (resp. columns). In such cases, we say that uncolored rows and columns use the *neutral color*. Examples of bidirectional colorings are displayed on Figure 1.3b.

With direct decompression for bidirectional Jacobian computation in mind, Hossain and Steihaug [30] elicit the constraint that every path on four vertices in the bipartite graph \mathcal{G}_b should use at least three colors, and deduce a simple greedy algorithm for bicoloring. Coleman and Verma [11] offer a more general treatment which also applies to decompression by substitution, by specifying that every cycle in \mathcal{G}_b should use at least three colors. Their algorithm includes a preprocessing step to decide which vertices could be left uncolored, which can be cast as an independent set problem. Gebremedhin et al. [20] compare both approaches and suggests connections with the theoretical framework developed for symmetric matrices. Goyal and Hossain [25] suggest an Integer Linear Programming (ILP) formulation. Juedes and Jones [32] propose a bicoloring algorithm with a guaranteed approximation ratio on the number of colors. Hossain and Steihaug [31] explore a new type of graph encoding which they claim is better suited to bidirectional approaches, but does not exhibit invariance by permutation. Xu and Coleman [46] generalize existing methods to account for other kinds of structure in the Jacobian (like repetition), as well as partial determination. Gaur et al. [19] give a new lower bound on the number of colors necessary for bicoloring and outline an intricate heuristic algorithm. Juedes and Jones [33] extend their previous study of approximation ratios and introduce new algorithms with performance guarantees. Finally, a recent paper by Gaur et al. [18] leverages a new ILP formulation with column generation to obtain good-quality solutions.

In terms of existing software implementations, `ColPack` [23] stands out because it was designed as a standalone matrix coloring library in C++, encompassing a wide variety of algorithms. That is why we choose it as our point of comparison. To the best of our knowledge, coloring tools are most often part of larger AD frameworks, integrated to enable sparse Jacobians and Hessians. `ColPack` itself interfaces with C/C++ AD toolkits like `ADOL-C` [27, 43], `CppAD` [2] or `ADIC2` [39, 40]. Sparse matrix coloring implementations for other languages include `ADMIT` [12], `ADiMAT` [44] and `MAD` [17] in MATLAB, `SparseDiffTools.jl` [24, 34] in Julia, `SparseHessianFD` [7] in R, `sparsejac` [42] in Python, as well as the domain-specific languages `CasADi` [1] and `JuMP.jl` [16, 37] for mathematical programming.

1.4. Contributions. This paper presents novel bicoloring algorithms, both with direct decompression and decompression via substitution. In contrast to previous approaches, our work builds on existing algorithms for star and acyclic coloring to address the bicoloring problem. Additionally, we propose a *post-processing* routine for symmetric colorings and bicolorings that aims to neutralize unneeded colors. In this context, we clarify the relationship between the neutral color and the use of two-colored stars and trees during the decompression of star and acyclic colorings. Implementation improvements are also described for star and acyclic coloring, as well as for decompression and vertex ordering.

We further introduce the Julia package `SparseMatrixColorings.jl`¹, which provides implementations of our new methods, along with improved versions of classical techniques for row, column, star, and acyclic colorings, as well as ordering and decompression routines. It was designed as an alternative to `ColPack` [23], written in a high-level programming language [4] with much fewer lines of code but nearly equivalent functionality and comparable speed.

2. Relation between bidirectional colorings and symmetric colorings.

Unlike unidirectional colorings, where an entry J_{ij} can only be directly recovered from the compressed row of its row's color (in row coloring) or the compressed column of its column's color (in column coloring), bidirectional colorings offer more flexibility by leveraging both colors. This enables more efficient recovery, both directly and through substitution. This flexibility is also present in symmetric colorings, where any entry H_{ij} in the lower triangular part ($i \geq j$) can be recovered from its symmetric counterpart H_{ji} in the upper triangular part. The symmetry relation $H_{ij} = H_{ji}$ thus allows leveraging color choices along both the row and column dimensions.

Building on this observation, we propose a new bidirectional coloring approach that reformulates the bicoloring problem as a symmetric coloring problem. To achieve this, we construct an *augmented matrix* H , where J is stored in the lower triangular portion and J^\top in the upper triangular portion. This formulation is given by:

$$(2.1) \quad H := \begin{bmatrix} 0 & J^\top \\ J & 0 \end{bmatrix}.$$

The adjacency graph \mathcal{G}_a of the augmented matrix H is exactly the same as the bipartite graph \mathcal{G}_b of the initial matrix J . With this representation, the symmetric colors assigned to the first n columns (or rows) of H determine the column colors of J , while those assigned to the last m columns (or rows) of H determine the row colors of J . Recovering J only requires decompressing the lower triangular portion

¹<https://github.com/gdalle/SparseMatrixColorings.jl>

of H , which is a standard procedure for symmetric matrices where only one triangle needs to be stored. This transformation allows us to extend the well-established symmetric coloring algorithms – such as star and acyclic coloring techniques – along with their associated decompression strategies and complexity properties developed by Gebremedhin et al. [21, 22] to the context of bicoloring. Figures 2.1a and 2.1b illustrate how a symmetric coloring of H translates into a bidirectional coloring of J , which exhibits a rectangular sparsity pattern. Note that a representation of adjoint graph in the context of hypergraphs [36] shares similarities with the structure of the augmented matrix (2.1).

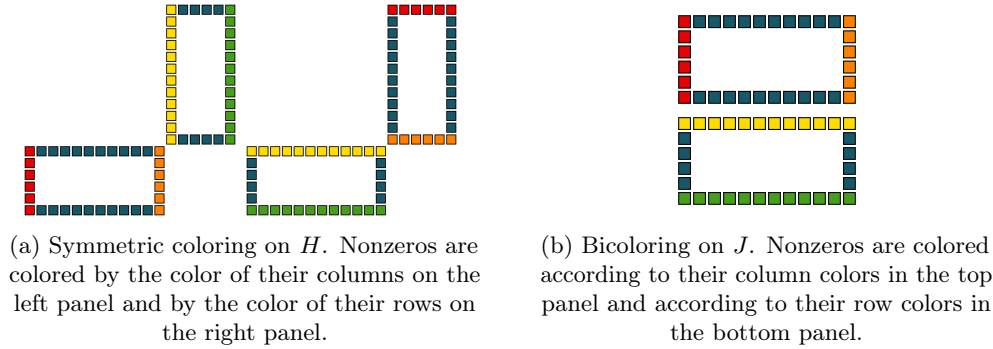


Fig. 2.1: Link between symmetric coloring and bicoloring

To preserve the mapping between the symmetric colors of H (stored as an integer vector `sym_colors`) and the row and column colors of J (stored as integer vectors `row_colors` and `col_colors`), we introduce two additional integer vectors: `sym_to_col` and `sym_to_row`. These vectors associate each symmetric color (numbered from 1 to `num_sym_colors`) with its corresponding column and row colors. If an entry in either `sym_to_col` (or `sym_to_row`) is 0, it signifies that the corresponding symmetric color is exclusively assigned to a subset of rows (or columns) in J . Additionally, we require that the row and column colors be consecutively numbered starting from 1. This contiguous indexing is crucial because each row or column index in the compressed matrices is directly related to a color. Maintaining this mapping simplifies the selection of seeds for AD and streamlines the decompression step. Algorithm 2.1 illustrates the algorithm used to compute the correspondence between the symmetric colors of H and the row and column colors of J .

Since our approach relies on symmetric colorings, the decompression routines require access to the compressed symmetric matrix B_s (or its transpose). B_s corresponds to the compression of the columns of H , grouped according to symmetric colors. Compressing by rows instead yields B_s^\top . Thanks to our mapping, explicitly constructing B_s is unnecessary. Each coefficient of B_s can be efficiently retrieved from B_r and B_c , where B_r stores the compressed rows of J , grouped by row colors, and B_c stores the compressed columns of J , grouped by column colors. The following holds:

$$(2.2) \quad B_s[r, c] = \begin{cases} B_r[\text{sym_to_row}[c], r] & \text{if } 1 \leq r \leq n \text{ and } \text{sym_to_row}[c] \neq 0, \\ B_c[r-n, \text{sym_to_col}[c]] & \text{if } 1 \leq r-n \leq m \text{ and } \text{sym_to_col}[c] \neq 0, \\ 0 & \text{otherwise.} \end{cases}$$

Bands of zeros in B_s that are not needed during decompression are not explicitly

Input:

- Two integers m and n corresponding to the number of rows and columns of J .
- An integer `num_sym_colors` representing the total number of symmetric colors.
- An integer array `sym_colors[1...(n+m)]` specifying a star or acyclic coloring.

Output:

- `row_colors[1...m]`: renumbered colors for rows.
- `col_colors[1...n]`: renumbered colors for columns.
- `sym_to_row[1...num_sym_colors]`: maps symmetric colors to row colors.
- `sym_to_col[1...num_sym_colors]`: maps symmetric colors to column colors.
- `num_row_colors`: number of colors for rows.
- `num_col_colors`: number of colors for columns.

```

1: sym_to_col[1...num_sym_colors] ← 0
2: col_colors[1...n] ← 0
3: num_col_colors ← 0
4: for j ← 1, ..., n do
5:   Let  $c_j \leftarrow \text{sym\_colors}[j]$ 
6:   if  $c_j > 0$  then
7:     if sym_to_col[ $c_j$ ] == 0 then
8:       num_col_colors ← num_col_colors + 1
9:       sym_to_col[ $c_j$ ] ← num_col_colors
10:    end if
11:    col_colors[j] ← sym_to_col[ $c_j$ ]
12:  end if
13: end for
14: sym_to_row[1...num_sym_colors] ← 0
15: row_colors[1...m] ← 0
16: num_row_colors ← 0
17: for i ← n+1, ..., n+m do
18:   Let  $c_i \leftarrow \text{sym\_colors}[i]$ 
19:   if  $c_i > 0$  then
20:     if sym_to_row[ $c_i$ ] == 0 then
21:       num_row_colors ← num_row_colors + 1
22:       sym_to_row[ $c_i$ ] ← num_row_colors
23:     end if
24:     row_colors[i-n] ← sym_to_row[ $c_i$ ]
25:   end if
26: end for

```

Algorithm 2.1: Procedure `remap_colors` for mapping symmetric colors to row and column colors. The arrays use 1-based indexing.

stored in B_r and B_c . They correspond to the structural zero blocks in H .

In Equation (2.1), we could have chosen to put J^\top in the lower triangular portion and J in the upper triangular portion instead. This switch is equally valid, and only requires minor adaptations in our algorithms. It would amount to reverting the order of vertices in the augmented adjacency graph \mathcal{G}_a obtained from the bipartite graph \mathcal{G}_b , listing row vertices first and column vertices next.

3. Post-processing.

3.1. Neutral color in symmetric and bidirectional colorings. We can see in Figures 2.1a and 2.1b that the dark blue color is unnecessary, so the rows and columns currently using it can be left uncolored instead, as illustrated in Figure 1.2. A neutral color indicates that the coefficients of neutralized columns or rows are not needed to recover all non-zeros. This is materialized by a blank square or triangle in our visualizations.

We developed a post-processing algorithm to reduce the number of colors by replacing some of them with a neutral color after applying symmetric colorings,

thereby also reducing the number of colors in our bicolorings. Thanks to symmetry, each off-diagonal entry can be recovered from either its row or its column, which are associated with different indices. In previous symmetric coloring approaches, every diagonal coefficient was assumed to be nonzero, making each color essential for diagonal retrieval and leaving no room for neutral colors. In contrast, for our bicoloring approach, all diagonal elements of H are zero, making post-processing beneficial. Note that our approach is not specific to the 2×2 block structure of H used for bicoloring. It can be applied to any symmetric matrix with at least some zeros on its diagonal and that has been colored using star or acyclic coloring.

After our post-processing, the non-neutral (i.e. colored) row and column vertices constitute a *vertex cover* of the corresponding graph (\mathcal{G}_a or \mathcal{G}_b). Indeed, every nonzero entry (edge in the graph) is incident to at least one colored vertex.

3.2. Relation between neutral color and two-colored structures. In graph theory, star and acyclic colorings are specialized forms of vertex colorings that impose additional constraints to prevent certain substructures within the graph. A star coloring is a proper vertex coloring where no path on four vertices uses two colors, meaning any path on four vertices uses at least three distinct colors. This restriction ensures that the subgraph induced by any two color structures forms a disjoint union of star graphs, thereby eliminating bicolored four-vertex paths. An acyclic coloring is a proper vertex coloring such that every cycle in the graph is colored with at least three colors, ensuring that no two-colored cycles exist. In other words, the subgraph induced by any two color structures is a forest, thereby eliminating bicolored cycles. Figure 3.1 illustrates the variants of two-colored structures encountered in star and acyclic colorings.

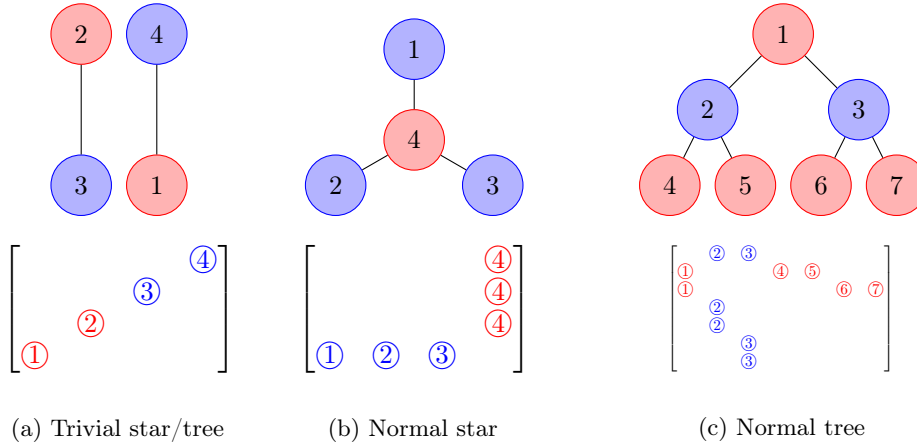


Fig. 3.1: Variants of two-colored structures with example matrices.

To determine if a color can be discarded, we need to identify cases where the color is not required during the decompression phase in star and acyclic colorings, which rely on two-colored structures. The first prerequisite for neutralizing a color in symmetric colorings is that it is not needed to recover diagonal coefficients. In the context of star coloring, only the color of the hubs of the stars is needed during decompression. The color of the spokes is not used (see the routine *DirectRecover2* in Gebremedhin et al. [22]). To illustrate this, consider an adjacency matrix J with one row and three

columns. The associated augmented matrix H is represented on [Figure 3.1b](#)): Here, the columns colored blue (spokes) are not used; only the column colored red (hub) is needed. Consequently, any color that does not appear in the hubs of any two-colored stars can safely be replaced by the neutral color.

In the context of acyclic coloring, only the color of the leaves in trees is not needed during decompression (see the routine *IndirectRecover* in [Gebremedhin et al. \[22\]](#)). However, for two-colored trees that are neither trivial nor standard two-colored stars (trees with a depth of at least 2), both colors must be retained as they correspond to the root and internal nodes (see the graph in [Figure 3.1c](#)). Therefore, the colors that can be neutralized in trees are those found in edges and stars (trees with a depth of 1).

The main challenge comes from edges, which are simplified forms of two-colored stars and trees that can be found in both star and acyclic colorings. In these cases, the color of either vertex can be used for decompression. For that reason, we suggest first processing all two-colored stars and trees with at least three vertices. Then, at the end of the procedure, we iterate over the remaining edges, leveraging our knowledge of nontrivial stars and trees. For each edge, if either of its two vertices is already (a) a hub of a normal two-colored star or (b) is simply a vertex in a normal two-colored tree, we cannot give it the neutral color. Thus, we choose to use that vertex for decompression of the current edge. Therein lies the benefit of processing individual edges at the end: if one color is already indispensable, we pick it for the hub, instead of making the other color indispensable too when it is not needed. On the other hand, if both colors can still be neutralized in the edge, we must arbitrarily neutralize one and then ensure that decompression uses the color of the other vertex. It may require updating who the hub is in these trivial two-colored structures.

For example, consider the following anti-diagonal matrix of [Figure 3.1a](#). We can remove either the blue or red color to compute all non-zeros. [Algorithm 3.1](#) summarizes the post-processing algorithm for star and acyclic colorings. Note that it can be simplified if we only use it for bicoloring, because H always has a diagonal of zeros, as well as in star coloring, because the set of normal two-colored trees \mathcal{T} is always empty.

Because an arbitrary choice may be necessary to neutralize one color in trivial two-colored structures, the total number of neutralized colors may vary. In the context of bicoloring, this choice can be made to reduce the number of colors in either the column partition or the row partition of a Jacobian. Depending on the shape of the Jacobian, as well as the cost of forward and reverse AD, one option may be more advantageous than the other.

3.3. Post-processing without color elimination. We recall that the post-processing aims to minimize the total number of colors, rather than maximizing the assignments of the neutral color. In some cases, the color assignments of rows and columns could be replaced with the neutral color without reducing the total number of distinct colors. This change affects only the seeds and does not benefit most AD tools. Tools like [Tapenade \[28\]](#) utilize activity analysis to identify active variables and skip computations on inactive ones. While this approach may optimize the process, further research is needed to determine if practical performance gains can be achieved. Additionally, this optimization could require different code being used to compute Ju and $J^T v$, depending on the seeds.

4. A new kind of coloring. In the symmetric setting, replacing some colors with the neutral color 0 means that the end result is no longer a standard star or acyclic coloring. We shed light on the resulting object in the case of star coloring only,

Input:

- An integer p corresponding to the dimension of a symmetric matrix H .
- An integer `num_sym_colors` representing the total number of symmetric colors.
- An integer array `sym_colors[1...p]` specifying a star or acyclic coloring.
- An integer array `offsets[1...p]` used as a workspace.
- A boolean vector `used[1...num_sym_colors]`: colors that can be neutralized.
- A set \mathcal{T} of normal two-colored trees.
- A set \mathcal{S} of normal two-colored stars.
- A set \mathcal{E} of trivial two-colored structures.

Output:

- The integer vector `sym_colors[1...p]` updated.

```

1: used[1...num_sym_colors] ← false
2: for  $k \leftarrow 1, \dots, p$  do
3:   if  $H_{k,k} \neq 0$  then
4:     used[sym_colors[k]] = true
5:   end if
6: end for
7: for each normal two-colored tree  $T$  in  $\mathcal{T}$  do
8:   Let  $i$  and  $j$  be the indices of two vertices connected by an edge in  $T$ 
9:   used[sym_colors[i]] = true
10:  used[sym_colors[j]] = true
11: end for
12: for each normal two-colored star  $S$  in  $\mathcal{S}$  do
13:   Let  $h$  be the index of the hub vertex in  $S$ 
14:   used[sym_colors[h]] = true
15: end for
16: for each trivial two-colored structure  $E$  in  $\mathcal{E}$  do
17:   Let  $i$  and  $j$  be the indices of the two vertices of the edge  $E$ 
18:   if used[sym_colors[i]] or used[sym_colors[j]] then
19:     Choose the hub  $h$  as  $i$  or  $j$  such that its color is used
20:   else
21:     Choose the hub  $h$  arbitrary between  $i$  and  $j$ 
22:     used[sym_colors[h]] = true
23:   end if
24: end for
25: num_neutral_colors ← 0
26: for  $c \leftarrow 1$  to num_sym_colors do
27:   if (not color_used[c]) then
28:     num_neutral_colors ← num_neutral_colors + 1
29:   else
30:     offsets[c] ← num_neutral_colors
31:   end if
32: end for
33: for  $i \leftarrow 1$  to  $p$  do
34:    $c \leftarrow \text{sym\_colors}[i]$ 
35:   if (not used[c]) then
36:     sym_color[i] ← 0
37:   else
38:     sym_color[i] ← sym_color[i] - offsets[c]
39:   end if
40: end for

```

Algorithm 3.1: Procedure `post_processing` for discarding colors after star and acyclic colorings. The arrays use 1-based indexing.

leaving acyclic coloring for future work.

4.1. Partition perspective. First, we recall the goal of coloring a symmetric matrix A with direct decomposition: obtaining a compressed representation from which every non-zero coefficient can be read directly. Following Gebremedhin et al.

[20, Definition 4.2], a *symmetrically orthogonal partition* of the columns of A is such that for every $A_{ij} \neq 0$, either (1) A_j is the only column in its group with a non-zero entry in row i , or (2) A_i is the only column in its group with a non-zero entry in row j . Coleman and Moré [10] prove that every star coloring of the adjacency graph of A induces a symmetrically orthogonal partition of the columns of A .

On the other hand, our post-processing method modifies the star coloring to induce a *neutralized symmetrically orthogonal partition*: it is such that for every $A_{ij} \neq 0$, either (1) A_j has a non-neutral color and is the only column in its group with a non-zero entry in row i , or (2) A_i has a non-neutral color and is the only column in its group with a non-zero entry in row j . We now give a graph characterization of this object in the special case where all diagonal coefficients of A are zero, which applies to the augmented matrix of (2.1). The usual star coloring corresponds to the opposite case where all diagonal coefficients are non-zero, which means the neutral color cannot be used. Intermediate cases where only some coefficients are non-zero may also be described, but the ensuing definitions are less crisp because the adjacency graph is not sufficient to distinguish between zero and non-zero diagonal entries (unless self-loops are considered).

4.2. Graph perspective. Let A be a symmetric $n \times n$ matrix whose diagonal entries are all zero. Let $\phi : \{1, \dots, n\} \rightarrow \{1, \dots, n\}$ be a mapping from the columns of A to integer colors. Any such mapping defines a partition P_ϕ of the columns of A , by gathering columns with the same color c inside a single group $P_\phi[c] := \{k \in \{1, \dots, n\} : \phi(k) = c\}$. As before, 0 denotes a neutral color, which is not used for recovery of the matrix. Let $\mathcal{G}_a = (\mathcal{V}, \mathcal{E})$ denote the adjacency graph of A , with vertex set $\mathcal{V} = \{1, \dots, n\}$ and edge set $\mathcal{E} = \{(i, j) : A_{ij} \neq 0\}$.

Definition. We say that ϕ is a *no-zig-zag coloring* of the adjacency graph \mathcal{G}_a if the following conditions are all met:

1. Every edge is incident on at least one colored vertex: if $(i, j) \in \mathcal{E}$, then $\phi(i) > 0$ or $\phi(j) > 0$.
2. Neutral-colored vertices have distinctly-colored neighbors: if j and q are adjacent to the same i such that $\phi(i) = 0$, then $\phi(j) \neq \phi(q)$.
3. There is no color-alternated (zig-zagging) path on four vertices: for any path (q, i, j, p) in \mathcal{G}_a , either $\phi(q) \neq \phi(j)$ or $\phi(i) \neq \phi(p)$, so that we cannot have a succession of colors of the form (c_1, c_2, c_1, c_2) .

Note that this definition does not require ϕ to be a coloring of \mathcal{G}_a in the usual sense: adjacent vertices are allowed to share the same non-neutral color $c > 0$. Therefore, no-zig-zag coloring is a relaxation of star coloring, as introduced by Coleman and Moré [10]. It is also related to star bicoloring, as introduced by Coleman and Verma [11].

Theorem. The mapping ϕ is a no-zig-zag coloring of \mathcal{G}_a if and only if the partition P_ϕ is a neutralized symmetrically orthogonal partition of the columns of A .

Before the formal proof, we give an intuitive way to obtain it. Given the matrix A below, we check which two-colored partitions allow recovery of A_{ij} (up to color switch). The results show that the only forbidden coloring pattern for path (q, i, j, p) is the zig-zag.

$A = \begin{pmatrix} \cdot & A_{qi} & \cdot & \cdot \\ A_{iq} & \cdot & A_{ij} & \cdot \\ \cdot & A_{ji} & \cdot & A_{jp} \\ \cdot & \cdot & A_{pj} & \cdot \end{pmatrix}$	q	i	j	p	recoverable A_{ij}
	c_1	c_2	c_1	c_2	no
	c_1	c_1	c_2	c_2	yes (in c_1 or c_2)
	c_1	c_2	c_2	c_1	yes (in c_2)
	c_1	c_1	c_1	c_2	yes (in c_1)
	c_1	c_1	c_2	c_1	yes (in c_2)

Proof. We tackle the two implications sequentially.

\Rightarrow Let ϕ define a no-zig-zag coloring of \mathcal{G}_a . If the partition P_ϕ is not a neutralized symmetrically orthogonal for A , there exists (i, j) such that $A_{ij} \neq 0$ cannot be recovered from i nor from j . This means we are in one of the following situations (the conditions refer to those defining the no-zig-zag coloring):

- $\phi(i) = 0$. By condition 1, $\phi(j) > 0$. Since A_{ij} cannot be recovered from j , there exists a column q with $A_{iq} \neq 0$ such that $\phi(q) = \phi(j)$. This violates condition 2.
- $\phi(j) = 0$. By condition 1, $\phi(i) > 0$. Since A_{ij} cannot be recovered from i , there exists a column p with $A_{jp} \neq 0$ such that $\phi(p) = \phi(i)$. This violates condition 2.
- $\phi(i) > 0$ and $\phi(j) > 0$. Since A_{ij} cannot be recovered from i nor from j , there exist q and p such that $A_{iq} \neq 0$, $A_{jp} \neq 0$, $\phi(i) = \phi(p)$ and $\phi(j) = \phi(q)$. But then the path (q, i, j, p) is color-alternated, which violates condition 3.

\Leftarrow Let P_ϕ be a neutralized symmetrically orthogonal partition for A . We now check the conditions of the no-zig-zag coloring one by one:

1. For $A_{ij} \neq 0$ to be recoverable, either $\phi(i) > 0$ or $\phi(j) > 0$ must hold. So the edge $(i, j) \in \mathcal{E}$ is incident on at least one colored vertex.
2. If $\phi(i) = 0$ and i has two neighbors j and q , then A_{ij} can only be recovered from j and A_{iq} from q . This implies that $\phi(j) \neq \phi(q)$.
3. Let (q, i, j, p) be a path in \mathcal{G}_a .
 - Assume $\phi(i) = 0$ (resp. $\phi(j) = 0$). Then, condition 2 imposes distinctly colored neighbors for i (resp. j). This brings the total number of colors to at least 3 and precludes a color-alternated path.
 - Now assume $\phi(i) > 0$ and $\phi(j) > 0$. Since A_{ij} is recoverable, this means that either $\phi(p) \neq \phi(i)$ or $\phi(q) \neq \phi(j)$. Thus, the path cannot be color-alternated either.

In the rest of the paper, even when our star and acyclic coloring algorithms are enhanced with post-processing, we still refer to them under the same name. This makes the comparison with previous versions more concise, in particular for benchmark tables. The reader should keep in mind that the actual object we obtain is a relaxation of the usual symmetric coloring concepts.

5. Software implementation. `SparseMatrixColorings.jl` (or `SMC` for short) is an open source library containing our new coloring algorithms, as well as some standard ones. It can be seen as a modernization of `ColPack` [23], written in a high-level language that facilitates applications. The implementation is based partly on a series of papers by the `ColPack` authors [20–23], but includes new algorithmic ideas. In particular, for bidirectional problems, `ColPack` only supports star bicoloring, while `SMC` includes our new acyclic bicoloring. As the benchmarks will demonstrate, this can lead to a smaller number of colors.

Furthermore, we fixed several bugs in `ColPack`, developed a C interface, and created a Julia wrapper `ColPack.jl`². The resulting fork³ of `ColPack` is made publicly available on GitHub.

5.1. Features and design. Like `ColPack`, our `SMC` package offers a variety of coloring and decompression options. It can compute either column, row or bidirectional

²<https://github.com/Exanauts/ColPack.jl>

³<https://github.com/amontoison/ColPack>

colorings, for symmetric or non-symmetric matrices, with direct or indirect decomposition. This translates into five different core algorithms: partial distance-2 coloring, star and acyclic coloring, and star and acyclic bicoloring. All of these algorithms employ greedy procedures that color vertices one after another. Since the order in which vertices are considered impacts the number of colors used, we allow users to select an ordering criterion: natural, random, largest first, dynamic largest first, smallest last, or incidence degree [23]. For each variant of the coloring problem, we only offer the most suitable model and leave alternative approaches aside. As an example, we provide a partial distance-2 coloring for bipartite graphs, but not distance-1 coloring on intersection graphs (which would be computationally more expensive [20]).

Thanks to our Julia implementation, **SMC** enjoys the benefits of just-in-time compilation and multiple dispatch [4]. Fast code is generated for a variety of input formats and number types, without needing to anticipate each one. At the same time, the use of a high-level language enables remarkable conciseness: according to `cloc`⁴, the entire package requires around 5 000 lines of Julia code, against nearly 30 000 lines of C++ for `ColPack`, with comparable functionalities.

5.2. Fast and flexible decompression. We took great care to optimize the performance of **SMC**, with a particular focus on decompression. Indeed, while coloring is usually performed just once, and then amortized over every subsequent Jacobian or Hessian computation, decompression is an integral part of derivative computations and often happens inside hot loops. Thus, the coloring step in **SMC** includes pre-allocation of necessary memory and pre-computation of relevant information, to make decompression as efficient as possible.

While **SMC** allows decompression into arbitrary matrices, it is most efficient when presented with sparse storage. Typical formats for sparse matrices include Compressed Sparse Column (CSC) or Compressed Sparse Row (CSR). The CSC format, which Julia considers the default, comprises three arrays:

- `nzval`, containing the nonzero values of the matrix, concatenated column-wise;
- `rowval`, containing the corresponding row indices, sorted in ascending order;
- `colptr`, an integer array of length $n + 1$ such that, for each column j , its nonzero entries appear in `nzval` and `rowval` at positions `colptr[j]` through `colptr[j+1]-1`. Accessing a single coefficient $A[i, j]$ in a CSC matrix A is expensive. It requires a binary search to find k on the sorted slice `colptr[j]:colptr[j+1]-1` such that `rowval[k] = i`, after which the requested value is read from or written to at `nzval[k]`. Thus, a naive unidirectional decompression $A[i, j] = B[i, \text{color}[j]]$ will be slower than it needs to be. That is why we precompute a vector of compressed indices such that `nzval[k] = B[compressed_indices[k]]`, where the matrix B is indexed linearly columnwise. With this preliminary step out of the way, decompression turns into a simple loop over all k in $1:\text{nnz}(A)$ without binary search. The computation of `compressed_indices` is a one-time cost and is quickly amortized when we need to perform multiple decompressions, as is the case in non-linear optimization methods that require many Jacobians and Hessians. It also allows decompression on SIMD architectures such as GPUs.

Anticipating cases where B itself might be too expensive to store, we also provide utilities for decompressing a single color at a time when it is feasible (which amounts to B having a single column or row). Similarly, in the case of symmetric matrices, we offer decompression inside a single triangle (lower or upper), thus skipping duplicate

⁴<https://github.com/AlDanial/cloc>

work. As noted earlier, decompression into a triangle for star and acyclic colorings is a crucial ingredient of our bidirectional decompression using the augmented matrix.

5.3. Performance considerations. In general, we found that the previously available pseudocode did not include all the necessary subtleties for efficient implementation of coloring and decompression algorithms. Therefore, we have listed some of these missing implementation details, as well as improvements we discovered, in [Appendix A](#). Notable performance optimizations include:

- Complete avoidance of hash tables for edge index management;
- Efficient reconstruction of 2-colored tree structures after acyclic coloring;
- Low-memory buckets for the dynamic degree-based orderings.

5.4. Integration with other tools. SMC integrates seamlessly with two other Julia packages: `SparseConnectivityTracer.jl`⁵ and `DifferentiationInterface.jl`⁶. The former provides utilities for sparsity pattern detection, a crucial step in the coloring process of Jacobians and Hessians, while the latter offers standardized access to various AD backends for computing JVPs, VJPs and HVPs. Together, these packages form a cohesive ecosystem for sparse AD in Julia [29].

With the upcoming release of Julia version 1.12, it will become possible to distribute small binaries and shared libraries of Julia packages. Then, we plan to create a C interface for SMC, aiming to improve its interoperability with other established AD systems such as ADOL-C [27] and CasADi [1].

6. Numerical experiments. We performed extensive numerical experiments comparing SMC with ColPack (or CP for short), both in terms of number of colors and in terms of runtime. Our test instances come from previous works: we reuse the nonsymmetric matrices from Gebremedhin et al. [23, Tables VI and VII], and the symmetric matrices from Gebremedhin et al. [20, Table 4.2]⁷. For the experiments below, we also include the Linear Programming and Harwell-Boeing matrices studied by Coleman and Verma [11, Tables 5.1 and 5.3]⁸. Statistics on the sizes of all the matrices used in our experiments are provided in [Table 6.1](#). We only present our main bicoloring results in this section, the rest of the tables can be found in [Appendix B](#).

[Table 6.2](#) compares the variants of bicoloring in ColPack and SMC in terms of the number of colors returned. It also reports the number of colors obtained by Coleman and Verma [11] with their bicoloring algorithm, referred to as CV, which we did not run ourselves. The variant of star bicoloring chosen for ColPack is `ImplicitCoveringStarBicoloring`, which was named as the best overall in Gebremedhin et al. [23]. For the star and acyclic bicoloring in SMC, the post-processing procedure is used. The boldfaced value indicates the lowest number of colors in each row.

As we can see, our acyclic bicoloring implementation (which enables decompression by substitution and was not available in ColPack) can give rise to fewer colors than implementations of star bicoloring in ColPack and SMC. Note however that these results are dependent on the chosen ordering: more details are given in [Appendix B](#). On most instances, the approach of Coleman and Verma [11] was found to yield fewer colors than SMC, yet their method has other drawbacks. For instance, it relies on partial

⁵<https://github.com/adrihill/SparseConnectivityTracer.jl>

⁶<https://github.com/JuliaDiff/DifferentiationInterface.jl>

⁷except `mrng1` and `mrng2`, which we did not find in the `SuiteSparse` collection

⁸except `boeing1` and `boeing2`, which we did not find in the `SuiteSparse` collection

group	name	sym	rows	cols	nnz
LPnetlib	lp_cre_a	false	3516	7248	18168
LPnetlib	lp_ken_11	false	14694	21349	49058
LPnetlib	lp_ken_13	false	28632	42659	97246
LPnetlib	lp_maros_r7	false	3136	9408	144848
LPnetlib	lp_cre_d	false	8926	73948	246614
LPnetlib	lp_ken_18	false	105127	154699	358171
Bai	af23560	false	23560	23560	484256
Shen	e40r0100	false	17281	17281	553562
vanHeukelum	cage11	false	39082	39082	559722
vanHeukelum	cage12	false	130228	130228	2032536
LPnetlib	lp_standata	false	359	1274	3230
LPnetlib	lp_scagr25	false	471	671	1725
LPnetlib	lp_scagr7	false	129	185	465
LPnetlib	lp_stair	false	356	614	4003
LPnetlib	lp_blend	false	74	114	522
LPnetlib	lp_vtp_base	false	198	346	1051
LPnetlib	lp_agg	false	488	615	2862
LPnetlib	lp_agg2	false	516	758	4740
LPnetlib	lp_agg3	false	516	758	4756
LPnetlib	lp_bore3d	false	233	334	1448
LPnetlib	lp_israel	false	174	316	2443
LPnetlib	lp_tuff	false	333	628	4561
LPnetlib	lp_adlitttle	false	56	138	424
HB	watt_2	false	1856	1856	11550
HB	can_256	true	256	256	2916
HB	can_268	true	268	268	3082
HB	can_292	true	292	292	2540
HB	can_634	true	634	634	7228
HB	can_715	true	715	715	6665
HB	can_1054	true	1054	1054	12196
HB	can_1072	true	1072	1072	12444
HB	impcol_c	false	137	137	411
HB	impcol_d	false	425	425	1339
HB	impcol_e	false	225	225	1308
HB	west0067	false	67	67	294
HB	west0381	false	381	381	2157
HB	west0497	false	497	497	1727
HB	gent113	false	113	113	655
HB	arc130	false	130	130	1282
DIMACS10	598a	true	110971	110971	1483868
DIMACS10	144	true	144649	144649	2148786
DIMACS10	m14b	true	214765	214765	3358036
DIMACS10	auto	true	448695	448695	6629222

Table 6.1: Structure and dimensions of the test matrices.

column- and row-intersection graphs (built from a partition of the matrix A into two sides), which can be denser than the original bipartite graph we use.

7. Conclusion. We presented new star and acyclic bicoloring algorithms for bidirectional compression-based computation of sparse Jacobian matrices. They allow the combined use of the forward and reverse modes of AD. We also presented accompanying efficient decompression procedures. Our bicoloring and decompression algorithms leverage the technology previously developed for sparse symmetric matrix (Hessian) computation. Our implementations are delivered via the Julia package `SparseMatrixColorings.jl`. This library also includes implementations of coloring and vertex ordering techniques for unidirectional computation of Jacobians (partial distance-2 coloring) and computation of Hessians (star and acyclic coloring). We showed

name	direct			substitution	
	CP	SMC	CV	SMC	CV
lp_cre_a	18	16		12	
lp_ken_11	6	5		4	
lp_ken_13	5	4		4	
lp_maros_r7	73	72		72	
lp_cre_d	17	15		13	
lp_ken_18	6	5		4	
af23560	44	32		45	
e40r0100	88	87		87	
cage11	82	81		79	
cage12	97	96		93	
lp_standata	11	10	9	8	7
lp_scagr25	10	9	8	5	5
lp_scagr7	10	9	8	5	5
lp_stair	39	38	36	35	29
lp_blend	18	17	16	14	14
lp_vtp_base	14	13	12	9	10
lp_agg	44	43	19	38	13
lp_agg2	44	43	26	38	21
lp_agg3	44	43	27	39	21
lp_bore3d	29	28	28	25	24
lp_israel	137	136	61	107	49
lp_tuff	27	25	21	26	16
lp_adlittle	12	11	11	11	10
watt_2	66	65	20	11	12
can_256	84	83	32	27	23
can_268	39	38	18	26	12
can_292	37	36	17	36	17
can_634	32	31	28	33	21
can_715	106	105	22	18	18
can_1054	37	36	31	25	23
can_1072	37	36	32	25	24
impcol_c	12	11	6	6	4
impcol_d	12	12	6	6	5
impcol_e	33	32	21	24	14
west0067	15	14	9	8	7
west0381	75	74	12	73	9
west0497	56	55	22	18	19
gent113	32	31	19	30	13
arc130	125	124	25	125	23

Table 6.2: Number of colors for bidirectional coloring with natural order, by decomposition mode and by package.

that **SMC** exhibits comparable performance with **ColPack** while offering additional features and reduced code complexity.

We conclude by pointing out a few directions for future work.

- As observed in our experiments, the number of colors obtained with our new bicoloring technique still compares unfavorably to the algorithm of [Coleman and Verma \[11\]](#). Understanding the cause of the difference in performance between the two approaches is an important challenge for further research.
- After the completion of the post-processing step (described in Section 3.1) that neutralizes unneeded colors, the rows and columns of the Jacobian that remain with non-neutral (actual) colors define a vertex cover in the bipartite graph view of the Jacobian. The characterization of this vertex cover in graph-theoretic terms is a worthy subject to investigate in future work.

- The augmented symmetric matrix for a non-symmetric matrix that we relied on for formulating our star and acyclic bicoloring is known in the literature as the adjoint graph representation of a hypergraph. It is worthwhile to explore this connection for studying hypergraph coloring problems.
- Our array-based implementation of the recovery routines associated with star and acyclic bicoloring naturally lends itself for parallelization within a SIMD framework. It will be interesting to exploit this to devise efficient GPU implementations.

Acknowledgements. Both first authors contributed equally.

We acknowledge the ideas and feedback contributed by Paul Hovland during the inception of this paper. We are grateful to Adrian Hill for his implementation of coloring visualization, and for his key role in shaping the sparse AD ecosystem in Julia through joint development efforts. We sincerely thank Jean-Baptiste Caillaud for his assistance in describing the applications in optimal control.

REFERENCES

- [1] J. A. E. Andersson, J. Gillis, G. Horn, J. B. Rawlings, and M. Diehl. CasADi: A software framework for nonlinear optimization and optimal control. *Mathematical Programming Computation*, 11(1):1–36, Mar. 2019. ISSN 1867-2957. DOI: [10.1007/s12532-018-0139-4](https://doi.org/10.1007/s12532-018-0139-4). URL <https://doi.org/10.1007/s12532-018-0139-4>.
- [2] B. M. Bell. CppAD: A package for C++ algorithmic differentiation. *Computational Infrastructure for Operations Research*, 57(10):3, 2012.
- [3] J. T. Betts. *Practical Methods for Optimal Control Using Nonlinear Programming, Third Edition*. SIAM, July 2020. ISBN 978-1-61197-619-9.
- [4] J. Bezanson, A. Edelman, S. Karpinski, and V. B. Shah. Julia: A Fresh Approach to Numerical Computing. *SIAM Review*, 59(1):65–98, Jan. 2017. ISSN 0036-1445, 1095-7200. DOI: [10.1137/141000671](https://epubs.siam.org/doi/10.1137/141000671). URL <https://epubs.siam.org/doi/10.1137/141000671>.
- [5] Å. Björck. *Numerical Methods for Least Squares Problems, Second Edition*. SIAM, July 2024. ISBN 978-1-61197-795-0.
- [6] M. Blondel and V. Roulet. The Elements of Differentiable Programming, July 2024. URL <http://arxiv.org/abs/2403.14606>.
- [7] M. Braun. sparseHessianFD: An R Package for Estimating Sparse Hessian Matrices. *Journal of Statistical Software*, 82(10), 2017. ISSN 1548-7660. DOI: [10.18637/jss.v082.i10](https://www.jstatsoft.org/v82/i10/). URL <http://www.jstatsoft.org/v82/i10/>.
- [8] T. F. Coleman and J.-Y. Cai. The Cyclic Coloring Problem and Estimation of Sparse Hessian Matrices. *SIAM Journal on Algebraic Discrete Methods*, 7(2):221–235, Apr. 1986. ISSN 0196-5212. DOI: [10.1137/0607026](https://epubs.siam.org/doi/abs/10.1137/0607026). URL <https://epubs.siam.org/doi/abs/10.1137/0607026>.
- [9] T. F. Coleman and J. J. Moré. Estimation of Sparse Jacobian Matrices and Graph Coloring Problems. *SIAM Journal on Numerical Analysis*, 20(1):187–209, Feb. 1983. ISSN 0036-1429. DOI: [10.1137/0720013](https://epubs.siam.org/doi/abs/10.1137/0720013). URL <https://epubs.siam.org/doi/abs/10.1137/0720013>.
- [10] T. F. Coleman and J. J. Moré. Estimation of sparse hessian matrices and graph coloring problems. *Mathematical Programming*, 28(3):243–270, Oct. 1984. ISSN 1436-4646. DOI: [10.1007/BF02612334](https://doi.org/10.1007/BF02612334). URL <https://doi.org/10.1007/BF02612334>.
- [11] T. F. Coleman and A. Verma. The Efficient Computation of Sparse Jacobian Matrices Using Automatic Differentiation. *SIAM Journal on Scientific Computing*, 19(4):1210–1233, Jan. 1998. ISSN 1064-8275. DOI: [10.1137/S1064827595295349](https://epubs.siam.org/doi/abs/10.1137/S1064827595295349). URL <https://epubs.siam.org/doi/abs/10.1137/S1064827595295349>.
- [12] T. F. Coleman and A. Verma. ADMIT-1: Automatic differentiation and MATLAB interface toolbox. *ACM Trans. Math. Softw.*, 26(1):150–175, Mar. 2000. ISSN 0098-3500. DOI: [10.1145/347837.347879](https://dl.acm.org/doi/10.1145/347837.347879). URL <https://dl.acm.org/doi/10.1145/347837.347879>.
- [13] T. F. Coleman, B. S. Garbow, and J. J. More. Software for estimating sparse Jacobian matrices. *ACM Transactions on Mathematical Software*, 10(3):329–345, Aug. 1984. ISSN 0098-3500. DOI: [10.1145/1271.1610](https://dl.acm.org/doi/10.1145/1271.1610). URL <https://dl.acm.org/doi/10.1145/1271.1610>.
- [14] A. R. Curtis, M. J. D. Powell, and J. K. Reid. On the Estimation of Sparse Jacobian Matrices. *IMA Journal of Applied Mathematics*, 13(1):117–119, Feb. 1974. ISSN 0272-4960. DOI: [10.1093/imamat/13.1.117](https://doi.org/10.1093/imamat/13.1.117). URL <https://doi.org/10.1093/imamat/13.1.117>.

- [15] T. A. Davis and Y. Hu. The university of Florida sparse matrix collection. *ACM Trans. Math. Softw.*, 38(1):1:1–1:25, Dec. 2011. ISSN 0098-3500. DOI: [10.1145/2049662.2049663](https://doi.org/10.1145/2049662.2049663). URL <https://doi.org/10.1145/2049662.2049663>.
- [16] I. Dunning, J. Huchette, and M. Lubin. JuMP: A Modeling Language for Mathematical Optimization. *SIAM Review*, 59(2):295–320, Jan. 2017. ISSN 0036-1445. DOI: [10/gftshn](https://epubs.siam.org/doi/abs/10.1137/15M1020575). URL <https://epubs.siam.org/doi/abs/10.1137/15M1020575>.
- [17] S. A. Forth. An efficient overloaded implementation of forward mode automatic differentiation in MATLAB. *ACM Transactions on Mathematical Software*, 32(2):195–222, June 2006. ISSN 0098-3500. DOI: [10.1145/1141885.1141888](https://dl.acm.org/doi/10.1145/1141885.1141888). URL <https://dl.acm.org/doi/10.1145/1141885.1141888>.
- [18] D. Gaur, S. Hossain, and R. R. Singh. Star Bicolouring of Bipartite Graphs. *Algorithms*, 17(9):377, Sept. 2024. ISSN 1999-4893. DOI: [10.3390/a17090377](https://www.mdpi.com/1999-4893/17/9/377). URL <https://www.mdpi.com/1999-4893/17/9/377>.
- [19] D. R. Gaur, S. Hossain, and A. Saha. Determining Sparse Jacobian Matrices Using Two-Sided Compression: An Algorithm and Lower Bounds. In J. Bélair, I. A. Frigaard, H. Kunze, R. Makarov, R. Melnik, and R. J. Spiteri, editors, *Mathematical and Computational Approaches in Advancing Modern Science and Engineering*, pages 425–434, Cham, 2016. Springer International Publishing. ISBN 978-3-319-30379-6. DOI: [10.1007/978-3-319-30379-6_39](https://doi.org/10.1007/978-3-319-30379-6_39).
- [20] A. H. Gebremedhin, F. Manne, and A. Pothen. What Color Is Your Jacobian? Graph Coloring for Computing Derivatives. *SIAM Review*, 47(4):629–705, Jan. 2005. ISSN 0036-1445. DOI: [10/cmwds4](https://epubs.siam.org/doi/abs/10.1137/S0036144504444711). URL <https://epubs.siam.org/doi/abs/10.1137/S0036144504444711>.
- [21] A. H. Gebremedhin, A. Tarafdar, F. Manne, and A. Pothen. New Acyclic and Star Coloring Algorithms with Application to Computing Hessians. *SIAM Journal on Scientific Computing*, 29(3):1042–1072, Jan. 2007. ISSN 1064-8275. DOI: [10.1137/050639879](https://epubs.siam.org/doi/abs/10.1137/050639879). URL <https://epubs.siam.org/doi/abs/10.1137/050639879>.
- [22] A. H. Gebremedhin, A. Tarafdar, A. Pothen, and A. Walther. Efficient Computation of Sparse Hessians Using Coloring and Automatic Differentiation. *INFORMS Journal on Computing*, 21(2):209–223, May 2009. ISSN 1091-9856. DOI: [10.1287/ijoc.1080.0286](https://pubsonline.informs.org/doi/abs/10.1287/ijoc.1080.0286). URL <https://pubsonline.informs.org/doi/abs/10.1287/ijoc.1080.0286>.
- [23] A. H. Gebremedhin, D. Nguyen, M. M. A. Patwary, and A. Pothen. ColPack: Software for graph coloring and related problems in scientific computing. *ACM Transactions on Mathematical Software*, 40(1):1:1–1:31, Oct. 2013. ISSN 0098-3500. DOI: [10.1145/2513109.2513110](https://dl.acm.org/doi/10.1145/2513109.2513110). URL <https://dl.acm.org/doi/10.1145/2513109.2513110>.
- [24] S. Gowda, Y. Ma, V. Churavy, A. Edelman, and C. Rackauckas. Sparsity Programming: Automated Sparsity-Aware Optimizations in Differentiable Programming. In *Program Transformations for ML Workshop at NeurIPS 2019*, Sept. 2019. URL <https://openreview.net/forum?id=rJIPdcY38B>.
- [25] M. Goyal and S. Hossain. Bi-Directional Determination of Sparse Jacobian Matrices: Approaches and Algorithms. *Electronic Notes in Discrete Mathematics*, 25:73–80, Aug. 2006. ISSN 1571-0653. DOI: [10.1016/j.endm.2006.06.091](https://www.sciencedirect.com/science/article/pii/S1571065306000722). URL <https://www.sciencedirect.com/science/article/pii/S1571065306000722>.
- [26] A. Griewank and A. Walther. *Evaluating Derivatives: Principles and Techniques of Algorithmic Differentiation*. Society for Industrial and Applied Mathematics, Philadelphia, PA, 2nd ed edition, 2008. ISBN 978-0-89871-659-7. URL <https://epubs.siam.org/doi/book/10.1137/1.9780898717761>.
- [27] A. Griewank, D. Juedes, and J. Utke. Algorithm 755: ADOL-C: A package for the automatic differentiation of algorithms written in C/C++. *ACM Transactions on Mathematical Software*, 22(2):131–167, June 1996. ISSN 0098-3500. DOI: [10.1145/229473.229474](https://dl.acm.org/doi/10.1145/229473.229474). URL <https://dl.acm.org/doi/10.1145/229473.229474>.
- [28] L. Hascoet and V. Pascual. The Tapenade automatic differentiation tool: Principles, model, and specification. *ACM Trans. Math. Softw.*, 39(3):20:1–20:43, May 2013. ISSN 0098-3500. DOI: [10.1145/2450153.2450158](https://dl.acm.org/doi/10.1145/2450153.2450158). URL <https://dl.acm.org/doi/10.1145/2450153.2450158>.
- [29] A. Hill and G. Dalle. Sparser, Better, Faster, Stronger: Efficient Automatic Differentiation for Sparse Jacobians and Hessians, Jan. 2025. URL <http://arxiv.org/abs/2501.17737>.
- [30] A. K. M. S. Hossain and T. Steihaug. Computing a sparse Jacobian matrix by rows and columns. *Optimization Methods and Software*, 10(1):33–48, Jan. 1998. ISSN 1055-6788. DOI: [10.1080/10556789808805700](https://doi.org/10.1080/10556789808805700). URL <https://doi.org/10.1080/10556789808805700>.
- [31] S. Hossain and T. Steihaug. Graph models and their efficient implementation for sparse Jacobian matrix determination. *Discrete Applied Mathematics*, 161(12):1747–1754, Aug. 2013. ISSN 0166-218X. DOI: [10.1016/j.dam.2012.12.010](https://www.sciencedirect.com/science/article/pii/S0166218X12004647). URL <https://www.sciencedirect.com/science/article/pii/S0166218X12004647>.
- [32] D. Juedes and J. Jones. Coloring Jacobians revisited: A new algorithm for star and acyclic bicoloring. *Optimization Methods and Software*, 27(2):295–309, Apr. 2012. ISSN 1055-6788. DOI: [10.1080/10556788.2011.606575](https://doi.org/10.1080/10556788.2011.606575). URL <https://doi.org/10.1080/10556788.2011.606575>.

- [33] D. W. Juedes and J. S. Jones. A generic framework for approximation analysis of greedy algorithms for star bicoloring. *Optimization Methods and Software*, 36(4):869–890, July 2021. ISSN 1055-6788. DOI: [10.1080/10556788.2019.1649671](https://doi.org/10.1080/10556788.2019.1649671). URL <https://doi.org/10.1080/10556788.2019.1649671>.
- [34] JuliaDiff contributors. JuliaDiff/SparseDiffTools.jl, Oct. 2024. URL <https://github.com/JuliaDiff/SparseDiffTools.jl>.
- [35] S. P. Kolodziej, M. Aznaveh, M. Bullock, J. David, T. A. Davis, M. Henderson, Y. Hu, and R. Sandstrom. The SuiteSparse Matrix Collection Website Interface. *Journal of Open Source Software*, 4(35):1244, Mar. 2019. ISSN 2475-9066. DOI: [10.21105/joss.01244](https://joss.theoj.org/papers/10.21105/joss.01244). URL <https://joss.theoj.org/papers/10.21105/joss.01244>.
- [36] X. T. Liu, J. Firoz, A. H. Gebremedhin, and A. Lumsdaine. NWHy: A Framework for Hypergraph Analytics: Representations, Data structures, and Algorithms. In *2022 IEEE International Parallel and Distributed Processing Symposium Workshops (IPDPSW)*, pages 275–284, May 2022. DOI: [10.1109/IPDPSW55747.2022.00057](https://ieeexplore.ieee.org/abstract/document/9835472). URL <https://ieeexplore.ieee.org/abstract/document/9835472>.
- [37] M. Lubin, O. Dowson, J. D. Garcia, J. Huchette, B. Legat, and J. P. Vielma. JuMP 1.0: Recent improvements to a modeling language for mathematical optimization. *Mathematical Programming Computation*, June 2023. ISSN 1867-2949, 1867-2957. DOI: [10.1007/s12532-023-00239-3](https://link.springer.com/10.1007/s12532-023-00239-3). URL <https://link.springer.com/10.1007/s12532-023-00239-3>.
- [38] S. T. McCormick. Optimal approximation of sparse hessians and its equivalence to a graph coloring problem. *Mathematical Programming*, 26(2):153–171, June 1983. ISSN 1436-4646. DOI: [10.1007/BF02592052](https://doi.org/10.1007/BF02592052). URL <https://doi.org/10.1007/BF02592052>.
- [39] S. H. K. Narayanan, B. Norris, and B. Winnicka. ADIC2: Development of a component source transformation system for differentiating C and C++. *Procedia Computer Science*, 1(1):1845–1853, May 2010. ISSN 1877-0509. DOI: [10.1016/j.procs.2010.04.206](https://www.sciencedirect.com/science/article/pii/S1877050910002073). URL <https://www.sciencedirect.com/science/article/pii/S1877050910002073>.
- [40] S. H. K. Narayanan, B. Norris, P. Hovland, D. C. Nguyen, and A. H. Gebremedhin. Sparse Jacobian Computation Using ADIC2 and ColPack. *Procedia Computer Science*, 4:2115–2123, Jan. 2011. ISSN 1877-0509. DOI: [10.1016/j.procs.2011.04.231](https://www.sciencedirect.com/science/article/pii/S1877050911002894). URL <https://www.sciencedirect.com/science/article/pii/S1877050911002894>.
- [41] M. J. D. Powell and Ph. L. Toint. On the Estimation of Sparse Hessian Matrices. *SIAM Journal on Numerical Analysis*, 16(6):1060–1074, Dec. 1979. ISSN 0036-1429. DOI: [10.1137/0716078](https://epubs.siam.org/doi/abs/10.1137/0716078). URL <https://epubs.siam.org/doi/abs/10.1137/0716078>.
- [42] M. Schubert. Mfschubert/sparsejac, Sept. 2024. URL <https://github.com/mfschubert/sparsejac>.
- [43] A. Walther. Getting Started with ADOL-C. *DROPS-IDN/v2/document/10.4230/DagSemProc.09061.10*, 2009. DOI: [10.4230/DagSemProc.09061.10](https://drops.dagstuhl.de/entities/document/10.4230/DagSemProc.09061.10). URL <https://drops.dagstuhl.de/entities/document/10.4230/DagSemProc.09061.10>.
- [44] J. Willkomm, C. H. Bischof, and H. M. Bücker. A new user interface for ADiMat: Toward accurate and efficient derivatives of MATLAB programmes with ease of use. *International Journal of Computational Science and Engineering*, 9(5-6):408–415, Jan. 2014. ISSN 1742-7185. DOI: [10.1504/IJCSE.2014.064526](https://www.inderscienceonline.com/doi/abs/10.1504/IJCSE.2014.064526). URL <https://www.inderscienceonline.com/doi/abs/10.1504/IJCSE.2014.064526>.
- [45] S. J. Wright. *Primal-Dual Interior-Point Methods*. SIAM, Jan. 1997. ISBN 978-1-61197-145-3.
- [46] W. Xu and T. F. Coleman. Efficient (Partial) Determination of Derivative Matrices via Automatic Differentiation. *SIAM Journal on Scientific Computing*, 35(3):A1398–A1416, Jan. 2013. ISSN 1064-8275. DOI: [10.1137/11085061X](https://epubs.siam.org/doi/abs/10.1137/11085061X). URL <https://epubs.siam.org/doi/abs/10.1137/11085061X>.

Appendix A. Implementation details.

We describe some implementation details for SMC, which improve or extend the algorithms presented in Gebremedhin et al. [20, 21, 22, 23]. The detailed pseudocode of every algorithm is given in Appendix C.

A.1. Graph storage.

A.1.1. Adjacency graph. The adjacency graph \mathcal{G}_a of a symmetric matrix A is stored as a Compressed Sparse Column (CSC) encoding with the help of two integer vectors `colptr` and `rowval`. We assume that the row indices in `rowval` are sorted in increasing order within each column, as is commonly done in sparse matrix libraries to facilitate traversal and efficient access. Note that by symmetry of A , it is also a Compressed Sparse Row (CSR) encoding of A . A minor issue is posed by non-zero diagonal coefficients: they may be present in the original matrix, but they are not

explicitly represented in the adjacency graph (which has no self-loops by definition). Thus, each iteration over neighbors of a vertex i must remember to skip i itself if encountered. Additionally, for star and acyclic colorings, we need a mapping from edges to unique integer indices. To achieve this, we construct a vector `edge_to_index` of the same length as the number of nonzeros in A , assigning a unique integer k to each edge (i, j) with $i \neq j$. In particular, this vector ensures that the off-diagonal entries of \hat{A} , a sparse CSC matrix defined by `colptr`, `rowval`, and `nzval=edge_to_index`, satisfy $\hat{A}_{ij} = \hat{A}_{ji} = k$. [Algorithm C.1](#) describes how to build this vector from the sparsity pattern of A . This approach is faster for grouped neighbor accesses than a container that stores unique key-value pairs $(i, j) \mapsto k$, such as a dictionary. Conversely, `ColPack` implements the mapping between edges and indices using a C++ `map`, which incurs additional overhead due to dynamic memory allocation and tree-based lookups. For the remainder of the algorithms, we regroup these three vectors into a structure called `adjacency_graph` and, for a given vertex v , we use the procedures `neighbors(adjacency_graph, v)` and `indexed_neighbors(adjacency_graph, v)` to return the neighbors (with the associated edge indices if needed) other than v .

A.1.2. Bipartite graph. For the bipartite graph \mathcal{G}_b , dual CSC and CSR encodings of A are necessary for optimal performance. The CSC version efficiently maps each column j to its row neighbors, and the CSR version efficiently maps each row i to its column neighbors. At the cost of twice the initial memory space (when A is not structurally symmetric), this allows efficient iteration over neighbors for both parts of the vertex space. To save memory, both CSC and CSR structures are manipulated without storing the nonzero values of A . [Algorithm C.2](#) details the conversion process between the CSC and CSR formats of A . We assume that row indices are sorted in increasing order within each column for the conversion.

A.2. Colorings.

A.2.1. Partial distance-2 coloring. We implement Algorithm 3.2 of [Gebremedhin et al. \[20\]](#) without any modification.

A.2.2. Star coloring. We implement Algorithm 4.1 of [Gebremedhin et al. \[21\]](#) without using hash tables, as detailed in [Algorithm C.3](#). The original algorithm did not assign a hub to trivial stars. However, the corresponding decompression routine requires that every star have a designated hub. To address this, we choose an arbitrary hub for trivial stars but encode it as a negative value $-h$. This convention not only makes trivial stars easily distinguishable from non-trivial ones during star coloring and post-processing but also simplifies the decompression process.

A.2.3. Acyclic coloring. We implement Algorithm 3.1 of [Gebremedhin et al. \[21\]](#) without using hash tables, as detailed in [Algorithm C.5](#). To efficiently build the 2-colored trees, we use a disjoint-set structure that requires two integer vectors `parents` and `ranks`, as well as an integer `nt` to keep track of the current number of trees. In the rest of the paper, this data structure is referred to as `forest`. Three essential routines are implemented on this structure: `create_forest`, `find_root` and `root_union`. They are detailed in [Algorithm C.4](#). Note that the edge index used to represent the root in the structure `forest` does not correspond to the actual tree root vertex. Instead, the selected “root” is maintained to minimize the tree’s height (i.e., it is chosen following a union-by-rank strategy to optimize path compression).

A.2.4. Star and acyclic bicoloring. To perform star and acyclic bicoloring, we build the adjacency graph of the augmented symmetric matrix H (2.1), derived from

a rectangular matrix J . This can be done by efficiently combining [Algorithm C.1](#) and [Algorithm C.2](#). To compute the seeds for the products Ju and $J^\top v$, we employ the vectors `row_colors` and `column_colors` produced by [Algorithm 2.1](#). Additionally, we use `sym_to_row` and `sym_to_col` (also generated by [Algorithm 2.1](#)) along with the relation (2.2) for decompression.

A.2.5. Post-processing. Detecting the trivial structures among the stars and trees is simple because we only need to check whether the number of vertices in each structure is exactly two (or one edge). However, in acyclic coloring, we need to distinguish the stars from the normal trees. To do that, we determine a boolean vector `is_star` that indicates for each tree whether it is a star (potentially trivial) or not. We can compute this concurrently with the reverse BFS orders of the two-colored trees ([Algorithm C.7](#)).

Note that we can reuse the vector `forbidden_colors` needed in both star and acyclic colorings (Algorithms 3.1 and 4.1 of [Gebremedhin et al. \[21\]](#)) for the vector `offsets` during post-processing ([Algorithm 3.1](#)).

A.3. Decompression. In SMC, we optimize the decompression of all our colorings for sparse CSC matrices with a generic fallback for matrices in other formats. Except for row and column coloring, where the decompression is straightforward, the decompression of symmetric colorings and derived bicolorings uses the algorithms *DirectRecover2* and *IndirectRecover* from [Gebremedhin et al. \[22\]](#), combined with new additional strategies.

A.3.1. Direct decompression. For direct decompression, we found it more efficient to use linear indexing and precompute the positions of nonzeros in the compressed matrix B . We store them in a dedicated vector `compressed_indices`.

$$\text{nzval}[k] = B[\text{compressed_indices}[k]] \quad \text{for } k = 1, \dots, \text{nnzA}.$$

For example, after column coloring, a coefficient A_{ij} is recovered from B_{ic} where $c = \text{col_colors}[j]$ at the linear index $(c - 1) \times m + i$ when B is column-ordered and 1-based indexed. Although the recovery is simple for row or column coloring, it becomes more complex and less parallel for star coloring and bicoloring. We need to use the stars to determine which vertex's color of an edge (i, j) is needed to recover a coefficient A_{ij} . Note that an additional integer vector `A_indices` is needed for star bicoloring to specify which nonzeros are recovered from B_r and B_c :

$$\begin{aligned} \text{nzval}[\text{A_indices}[k]] &= B_c[\text{compressed_indices}[k]], \quad \text{for } k = 1, \dots, \ell, \\ \text{nzval}[\text{A_indices}[k]] &= B_r[\text{compressed_indices}[k]], \quad \text{for } k = \ell + 1, \dots, \text{nnzA}. \end{aligned}$$

The variable ℓ denotes the number of nonzeros of A recovered from B_c .

A.3.2. Decompression by substitution. For acyclic coloring and bicoloring, the decompression step relies on traversing the two-colored trees. However, existing work does not explain how to reconstruct the structure of these trees from their disjoint-set representation. While the coloring phase identifies which edges belong to the same tree, it does not reveal how each tree can be traversed from its leaves to its root, following a reverse breadth-first search (BFS) order. Our goal is to clarify how this ordering can be computed and extracted from the structure `forest`. Once determined, the edges within each tree are sorted according to the order in which they must be processed.

In this ordering, each edge is oriented so that its first vertex is a leaf (after pruning previously processed edges), and its second vertex is an internal node. This convention enables the direct application of *IndirectRecover* from Gebremedhin et al. [22].

The reconstruction of the trees is described in Algorithm C.6, and the computation of the reverse BFS order is presented in Algorithm C.7. We use the fact that a tree with `ne` edges has exactly `ne+1` vertices in these routines. Note that the vector `ranks` from the structure `forest` can be repurposed to store `root_to_tree` in Algorithm C.6. Likewise, the array `first_visit_to_tree` used during acyclic coloring can be reused to store `reverse_bfs_orders` in Algorithm C.7.

With this approach, the decompression of each tree can be performed in parallel. However, it offers less parallelism than direct decompression, since parallelism occurs across the number of trees rather than across the number of nonzeros. Moreover, the number of edges per tree may vary significantly, which may require load balancing to efficiently exploit this parallelism.

For this reason, we emphasize that *IndirectRecover* from Gebremedhin et al. [22] is equivalent to solving a sparse triangular system in which all coefficients are either 0 or 1, the unknowns correspond to the nonzeros, and the right-hand side is a subset of the entries of the matrix B . An alternative is to explicitly compute the inverses of all the sparse triangular matrices needed. These inverses remain triangular and contain only -1 (off-diagonal), 0, and 1 (diagonal) as entries. All of these inverse matrices can then be assembled into a single large sparse matrix, and the full vector of `nzval` can be recovered through a single sparse matrix-vector multiplication with $B[\text{compressed_indices}]$. This approach might require significantly more storage, but it is likely the most efficient way to exploit SIMD architectures such as GPUs.

A.4. Vertex orderings. Our implementation of vertex orderings follows Section 5.1 of Gebremedhin et al. [23]. The authors describe three different orderings using a common framework, that of dynamic degree-based orderings. Each vertex in the graph gets assigned a dynamic degree, which evolves as the ordering progresses and the permutation π of vertices gets built. More precisely, the back degree of a vertex v is the number of neighbors that appear before v in the permutation π , while the forward degree of v is the number of neighbors that appear after v . As the permutation $\pi = \{v_1, \dots, v_n\}$ is grown iteratively, either from v_1 to v_n or from v_n to v_1 , the dynamic degrees (back or forward) evolve. Since these degrees are used to select which vertex will be added to the permutation next, we need an efficient way to keep track of them.

Gebremedhin et al. [23, Figure 2] propose a bucket sort mechanism to achieve this goal. They use one variable-size bucket per possible value of the dynamic degree. Whenever the dynamic degree of a vertex changes, it gets moved one bucket up or one bucket down, and appended to the end of the destination bucket. This is rather straightforward to implement, but requires one stack-like data structure per bucket, whose size will increase or decrease and cannot be predicted ahead of time.

To improve memory locality and remove the need for variable-sized containers, we suggest an alternative where all buckets are stored inside the same vector, and the limits of each bucket (an interval of integers) are kept updated separately. The key is to allow modification of a bucket either from the start or from the end. That way, when a vertex v moves up from bucket d to bucket $d + 1$, bucket d shrinks from the right and bucket $d + 1$ grows to the left. When a vertex v moves down from bucket d to bucket $d - 1$, bucket d shrinks from the left and bucket $d - 1$ grows to the right. In both cases, the total amount of storage necessary remains constant and predictable.

The two algorithms are detailed and compared in Algorithm C.8 and Algorithm C.9,

on the special case of a vertex whose dynamic degree needs to increase by one.

Appendix B. Benchmarks.

B.1. Setup. The benchmarks are run on a 14-inch MacBook Pro M3 (2023) with 36 GB of RAM, using Julia v1.11.5 in single-threaded mode. `SMC` is called through its native Julia interface, which accepts CSC matrices, while `ColPack` is called through its command line interface, which accepts `.mtx` matrix files. We use a compiled version of `ColPack` without OpenMP (through `ColPack.jl` v0.5.0), along with `SparseMatrixColorings.jl` v0.4.19.

B.2. Test matrices. The test matrices are retrieved from the SuiteSparse matrix collection [15, 35]. We describe their main features in [Table 6.1](#).

B.3. Number of colors. We first investigate whether or not our `SMC` implementation is consistent with the results returned by `ColPack`. This is done for each of the following orders: smallest last (SL), incidence degree (ID), largest first (LF), dynamic largest first (DLF) and natural (N). Boldfaced numbers indicate the minimum number of colors for a given instance across all orders.

We recall that some implementation differences between `SMC` and `ColPack` can affect the number of colors:

- `SMC` has a completely different algorithm for star bicoloring ([Section 2](#));
- The natural order for bicoloring differs: `SMC` colors columns before rows, whereas `ColPack` does the opposite;
- `SMC` calls a post-processing routine after star and acyclic coloring algorithms ([Section 3](#)), which can reduce the number of colors if some diagonal coefficients are zero.

To minimize discrepancies, we always imitate `ColPack`'s stack-based ordering algorithm instead of leveraging our own vector-based improvement ([Appendix A.4](#)).

B.3.1. Unidirectional and symmetric colorings. Results for row coloring are presented in [Table B.1](#), for column coloring in [Table B.2](#), for star coloring in [Table B.3](#), for acyclic coloring in [Table B.4](#). In these four tables, underlined numbers indicate a discrepancy between `SMC` and `ColPack`. Each table contains at most one instance where the two libraries differ (usually by a couple of colors), which suggests that both implementations give very similar results.

name	SL		ID		LF		DLF		N	
	CP	SMC	CP	SMC	CP	SMC	CP	SMC	CP	SMC
lp_cre_a	14	14	14	14	14	14	14	14	16	16
lp_ken_11	4	4	4	4	4	4	5	5	5	5
lp_ken_13	4	4	5	5	5	5	5	5	4	4
lp_maros_r7	80	80	88	88	100	100	113	113	72	72
lp_cre_d	15	15	15	15	13	13	14	14	15	15
lp_ken_18	4	4	5	5	5	5	5	5	5	5
af23560	42	42	43	42	43	36	60	59	43	32
e40r0100	70	70	71	71	85	85	86	86	87	87
cage11	64	64	67	67	67	67	70	70	81	81
cage12	67	67	72	72	73	73	79	79	96	96

Table B.1: Number of colors for row coloring.

B.3.2. Bidirectional colorings. Results for star bicoloring are presented in [Table B.5](#), and for acyclic bicoloring in [Table B.6](#). Here, we observe that the lowest

name	SL		ID		LF		DLF		N	
	CP	SMC	CP	SMC	CP	SMC	CP	SMC	CP	SMC
lp_cre_a	360	360	360	360	360	360	360	360	360	360
lp_ken_11	125	125	124	124	128	128	122	122	130	130
lp_ken_13	171	171	171	171	174	174	170	170	176	176
lp_maros_r7	83	83	90	90	70	70	114	114	74	74
lp_cre_d	808	808	808	808	808	808	808	808	813	813
lp_ken_18	325	325	326	326	328	328	325	325	330	330
af23560	42	42	42	42	43	44	59	59	44	32
e40r0100	70	70	71	71	87	87	85	85	95	95
cage11	64	64	67	67	67	67	70	70	81	81
cage12	67	67	72	72	73	73	79	79	96	96

Table B.2: Number of colors for column coloring.

name	SL		ID		LF		DLF		N	
	CP	SMC	CP	SMC	CP	SMC	CP	SMC	CP	SMC
598a	23	23	23	23	27	27	28	28	28	28
144	24	24	25	25	28	28	30	30	29	29
m14b	28	28	27	27	36	36	38	38	32	32
auto	27	27	28	<u>29</u>	36	36	34	34	32	32

Table B.3: Number of colors for star coloring.

name	SL		ID		LF		DLF		N	
	CP	SMC	CP	SMC	CP	SMC	CP	SMC	CP	SMC
598a	12	12	12	<u>11</u>	12	12	12	12	13	13
144	13	13	13	13	13	13	14	14	14	14
m14b	14	14	14	14	15	15	16	16	18	18
auto	14	14	15	15	15	15	16	16	16	16

Table B.4: Number of colors for acyclic coloring.

number of colors is nearly always provided by an **SMC** implementation, and that acyclic bicoloring leads to fewer colors than star bicoloring, as expected. In both star and acyclic bicoloring, the number of colors produced by the **SMC** implementation is heavily dependent on the ordering, and some orderings perform very poorly. We conjecture that this may be due to the orderings being applied to the augmented symmetric matrix, whereas they were designed for a different graph representation. Designing orderings suitable for the **SMC** approach is an interesting direction for future research.

name	SL		ID		LF		DLF		N	
	CP	SMC	CP	SMC	CP	SMC	CP	SMC	CP	SMC
lp_cre_a	27	31	24	370	23	364	21	365	18	16
lp_ken_11	128	68	129	128	8	134	5	133	6	5
lp_ken_13	176	166	177	169	8	180	6	182	5	4
lp_maros_r7	131	80	153	91	130	134	71	116	73	72
lp_cre_d	38	275	25	815	23	811	17	810	17	15
lp_ken_18	331	241	331	332	8	334	6	337	6	5
af23560	75	53	74	77	67	71	51	105	44	32
e40r0100	99	155	98	72	93	83	89	147	88	87
cage11	96	76	105	81	94	87	69	158	82	81
cage12	102	106	114	90	104	97	74	121	97	96

Table B.5: Number of colors for star bicoloring.

name	SL SMC	ID SMC	LF SMC	DLF SMC	N SMC
lp_cre_a	43	118	116	117	12
lp_ken_11	10	11	12	12	4
lp_ken_13	10	10	11	10	4
lp_maros_r7	159	97	115	115	72
lp_cre_d	87	152	151	148	13
lp_ken_18	10	10	9	10	4
af23560	60	61	57	87	45
e40r0100	157	72	83	148	87
cage11	46	45	52	125	79
cage12	47	45	55	99	93

Table B.6: Number of colors for acyclic bicoloring (SMC only).

B.4. Timings. We have established that the SMC and ColPack algorithms are, at minimum, directly comparable. The next question is one of performance: can a Julia implementation compete with the speed of an optimized C++ library? To answer it, we run the function of interest five times and record the minimum runtime for each package. Then, we display the ratio of these minimum runtimes, SMC over ColPack. Ratios under 1 indicates that SMC is faster, while ratios above 1 show that ColPack stays ahead. We do not measure the time it takes to process the matrix and construct the graph (which is format-dependent): we only measure the ordering time and the subsequent coloring time once the graph is available.

B.4.1. Coloring times. We start with the results for coloring times in the case of the natural order, presented in [Table B.7](#) and [Table B.8](#). The unidirectional colorings in SMC are generally as fast as ColPack's, but our symmetric and bidirectional colorings can be up to four times faster. The slight overhead in the unidirectional routines stems from Julia's bounds checking on array accesses, an operation not present in C++, which may modestly constrain compiler optimizations. Note that for acyclic bicoloring, we compute the runtime ratio compared to ColPack's star bicoloring, for lack of an equivalent algorithm.

name	column	row	bidirectional*	
			star	acyclic
lp_cre_a	1.2	0.808	0.27	0.563
lp_ken_11	1.11	1.08	0.202	0.424
lp_ken_13	1.17	1.08	0.22	0.405
lp_maros_r7	0.899	1.13	0.568	1.22
lp_cre_d	1.37	1.16	0.227	0.497
lp_ken_18	1.22	1.22	0.201	0.442
af23560	1.35	1.43	0.377	0.973
e40r0100	1.17	1.31	0.615	1.22
cage11	1.23	1.28	0.414	1.2
cage12	1.28	1.33	0.393	1.28

Table B.7: Coloring time ratios (SMC/ColPack) for row coloring, column coloring and bicoloring with natural order.

* both compared to star bicoloring in ColPack

name	unidirectional	
	star	acyclic
598a	0.271	0.449
144	0.267	0.455
m14b	0.277	0.449
auto	0.304	0.489

Table B.8: Coloring time ratios (SMC/ColPack) for star and acyclic coloring with natural order.

B.4.2. Ordering times. We present results for the ordering subroutines in [Table B.9](#), [Table B.10](#), and [Table B.11](#). As we can see, SMC is usually within a factor of

2 of **ColPack**'s ordering performance. Note that for bicoloring, **SMC** runs the ordering on the augmented adjacency graph, while **ColPack** runs it on the initial bipartite graph, which makes the timings harder to compare meaningfully.

name	SL	ID	LF	DLF
lp_cre_a	0.83	1.04	0.84	1.06
lp_ken_11	1.18	1.49	1.57	1.35
lp_ken_13	1.16	1.37	1.63	1.39
lp_maros_r7	1.3	1.34	1.4	0.91
lp_cre_d	1.11	1.18	1.04	1.24
lp_ken_18	1.22	1.47	1.97	1.37
af23560	1.46	1.73	1.89	1.05
e40r0100	0.87	0.97	1.21	0.86
cage11	1.17	1.19	1.2	1.22
cage12	1.24	1.23	1.29	1.31

Table B.9: Ordering time ratios
(**SMC/ColPack**) for row coloring.

name	SL	ID	LF	DLF
lp_cre_a	1.36	0.91	1.86	1.42
lp_ken_11	1.82	1.29	2.41	1.46
lp_ken_13	1.57	1.28	2.48	1.58
lp_maros_r7	1.38	1.22	1.36	0.94
lp_cre_d	1.64	1.39	1.58	1.58
lp_ken_18	1.78	1.41	2.94	1.71
af23560	1.5	1.7	1.7	1
e40r0100	0.95	1	1.28	0.95
cage11	1.18	1.08	1.19	1.24
cage12	1.24	1.12	1.26	1.31

Table B.10: Ordering time ratios
(**SMC/ColPack**) for column coloring.

name	SL	ID	LF	DLF
598a	1.71	1.68	4.96	1.59
144	1.76	1.74	5.81	1.9
m14b	1.84	1.67	5.89	1.97
auto	1.94	1.83	7.41	1.73

Table B.11: Ordering time ratios
(**SMC/ColPack**) for star coloring.

Appendix C. Pseudocode.

In this appendix, we present the detail of the algorithms we adapted or designed for ordering, coloring and decompression.

Input:

- An integer `n` corresponding to the dimension of a symmetric matrix A .
- An integer `nnzA` corresponding to the number of non-zeros of A .
- An integer vector `colptr` of length $n+1$.
- An integer vector `rowval` of length `nnzA`.
- An integer vector `offsets` of length n .

Output:

- An integer vector `edge_to_index` of length `nnzA`.

```

1: Initialize offsets[1...n]  $\leftarrow 0$ 
2: Set k  $\leftarrow 0$ 
3: for j  $\leftarrow 1$  to n do
4:   for p  $\leftarrow \text{colptr}[j]$  to colptr[j+1]-1 do
5:     i  $\leftarrow \text{rowval}[p]$ 
6:     if i  $> j$  then
7:       k  $\leftarrow k + 1$ 
8:       edge_to_index[p]  $\leftarrow k$ 
9:       q  $\leftarrow \text{colptr}[i] + \text{offsets}[i]$ 
10:      edge_to_index[q]  $\leftarrow k$ 
11:      offsets[i]  $\leftarrow \text{offsets}[i] + 1$ 
12:    end if
13:  end for
14: end for
15: return edge_to_index
```

Algorithm C.1: Procedure to build the vector `edge_to_index` from a sparse symmetric matrix A stored in CSC format, where the entries in `rowval` for each column must be sorted in ascending order. The arrays use 1-based indexing.

Input:

- An integer m corresponding to the number of rows of A .
- An integer n corresponding to the number of columns of A .
- An integer $nnzA$ corresponding to the number of non-zeros of A .
- An integer vector $colptr$ of length $n+1$.
- An integer vector $rowval$ of length $nnzA$.

Output:

- An integer vector $rowptr$ of length $m+1$.
- An integer vector $colval$ of length $nnzA$.

```

1: Initialize  $rowptr[1..m+1] \leftarrow 0$ 
2: for  $k \leftarrow 1$  to  $nnzA$  do
3:    $i \leftarrow rowval[k]$ 
4:    $rowptr[i] \leftarrow rowptr[i] + 1$ 
5: end for
6: Set  $counter \leftarrow 1$ 
7: for  $i \leftarrow 1$  to  $m$  do
8:    $nnz\_row \leftarrow rowptr[i]$ 
9:    $rowptr[i] \leftarrow counter$ 
10:   $counter \leftarrow counter + nnz\_row$ 
11: end for
12:  $rowptr[m+1] \leftarrow counter$ 
13: for  $j \leftarrow 1$  to  $n$  do
14:   for  $p \leftarrow colptr[j]$  to  $colptr[j+1]-1$  do
15:      $i \leftarrow rowval[p]$ 
16:      $pos \leftarrow rowptr[i]$ 
17:      $colval[pos] \leftarrow j$ 
18:      $rowptr[i] \leftarrow rowptr[i] + 1$ 
19:   end for
20: end for
21: for  $i \leftarrow m$  down to  $2$  do
22:    $rowptr[i] \leftarrow rowptr[i-1]$ 
23: end for
24:  $rowptr[1] \leftarrow 1$ 
25: return  $rowptr, colval$ 

```

Algorithm C.2: Procedure to convert a sparse matrix A stored in CSC format ($colptr, rowval$) into its equivalent CSR representation ($rowptr, colval$). The arrays use 1-based indexing.


```

Input:
  • adjacency_graph, vertices_in_order, nv, ne
Output:
  • color, star, hub
1: color[1,...,nv]  $\leftarrow$  0
2: forbidden_colors[1,...,nv]  $\leftarrow$  0
3: first_neighbor[1,...,nv]  $\leftarrow$  (0,0,0)
4: treated[1,...,nv]  $\leftarrow$  0
5: star[1,...,ne]  $\leftarrow$  0
6: hub  $\leftarrow$  []
7: num_stars  $\leftarrow$  0
8: for each  $v \in \text{vertices\_in\_order}$  do
9:   for each  $(w, \text{index\_vw}) \in \text{indexed\_neighbors}(\text{adjacency\_graph}, v)$  do
10:    if color[w]  $\neq$  0 then
11:      forbidden_colors[color[w]]  $\leftarrow$  v
12:       $(p, q, \text{index\_pq}) \leftarrow \text{first\_neighbor}[\text{color}[w]]$ 
13:      if  $p == v$  then
14:        if treated[q]  $\neq$  v then
15:          for each  $x \in \text{neighbors}(\text{adjacency\_graph}, q)$  do
16:            if color[x]  $\neq$  0 then
17:              forbidden_colors[color[x]]  $\leftarrow$  v
18:            end if
19:          end for
20:          treated[q]  $\leftarrow$  v
21:        end if
22:        for each  $x \in \text{neighbors}(\text{adjacency\_graph}, w)$  do
23:          if color[x]  $\neq$  0 then
24:            forbidden_colors[color[x]]  $\leftarrow$  v
25:          end if
26:        end for
27:        treated[w]  $\leftarrow$  v
28:      else
29:        first_neighbor[color[w]]  $\leftarrow$  (v, w, index_vw)
30:        for each  $(x, \text{index\_wx}) \in \text{indexed\_neighbors}(\text{adjacency\_graph}, w)$  do
31:          if  $x \neq v$  and color[x]  $\neq$  0 and  $x == \text{hub}[\text{star}[\text{index\_wx}]]$  then
32:            forbidden_colors[color[x]]  $\leftarrow$  v
33:          end if
34:        end for
35:      end if
36:    end if
37:  end for
38: color[v]  $\leftarrow \min\{i \mid \text{forgiven\_colors}[i] \neq v\}$ 
39: for each  $(w, \text{index\_vw}) \in \text{indexed\_neighbors}(\text{adjacency\_graph}, v)$  do
40:   if color[w]  $\neq$  0 then
41:     x_exists  $\leftarrow$  false
42:     for each  $(x, \text{index\_wx}) \in \text{indexed\_neighbors}(\text{adjacency\_graph}, w)$  do
43:       if  $x \neq v$  and color[x] == color[v] then
44:         star_wx  $\leftarrow$  star[index_wx]
45:         hub[star_wx]  $\leftarrow$  w
46:         star[index_vw]  $\leftarrow$  star_wx
47:         x_exists  $\leftarrow$  true
48:       break
49:     end if
50:   end for
51:   if (not x_exists) then
52:      $(p, q, \text{index\_pq}) \leftarrow \text{first\_neighbor}[\text{color}[w]]$ 
53:     if  $p == v$  and  $q \neq w$  then
54:       star_vq  $\leftarrow$  star[index_pq]
55:       hub[star_vq]  $\leftarrow$  v
56:       star[index_vw]  $\leftarrow$  star_vq
57:     else
58:       num_stars  $\leftarrow$  num_stars + 1
59:       push!(hub, -v) or push!(hub, -w)
60:       star[index_vw]  $\leftarrow$  num_stars
61:     end if
62:   end if
63: end if
64: end for
65: end for

```

Algorithm C.3: Procedure star_coloring.

```

Procedure create_forest(ne)
• Input: An integer ne corresponding to the number of edges.
• Output: A structure forest.
1: nt  $\leftarrow$  ne
2: parents[1..ne]  $\leftarrow$  [1, 2, ..., ne]
3: ranks[1..ne]  $\leftarrow$  [0, 0, ..., 0]

Procedure find_root(forest, index)
• Input: One edge index, index, and the structure forest.
• Output: The root of the tree containing index.
1: if parents[index]  $\neq$  index then
2:   parents[index]  $\leftarrow$  find_root(parents[index], forest)
3: end if
4: return parents[index]

Procedure root_union(forest, root1, root2)
• Input: Two root indices, root1 and root2, and the structure forest.
• Output: The structure forest after merging the trees with roots root1 and root2.
1: if ranks[root1] < ranks[root2] then
2:   (root1, root2)  $\leftarrow$  (root2, root1)
3: else if ranks[root1] == ranks[root2] then
4:   ranks[root1]  $\leftarrow$  ranks[root1] + 1
5: end if
6: parents[root2]  $\leftarrow$  root1
7: nt  $\leftarrow$  nt - 1

```

Algorithm C.4: Routines related the structure *forest*.

```

Input:
  • adjacency_graph, vertices_in_order, nv, ne
Output:
  • color, forest
1: color[1,...,nv]  $\leftarrow$  0
2: forbidden_colors[1,...,nv]  $\leftarrow$  0
3: first_neighbor[1,...,nv]  $\leftarrow$  (0,0,0)
4: first_visit_to_tree[1,...,ne]  $\leftarrow$  (0,0)
5: forest  $\leftarrow$  create_forest(ne)
6: for each  $v \in$  vertices_in_order do
7:   for each  $(w, \text{index\_vw}) \in$  indexed_neighbors(adjacency_graph, v) do
8:     if color[w]  $\neq$  0 then
9:       forbidden_colors[color[w]]  $\leftarrow$  v
10:    end if
11:  end for
12:  for each  $w \in$  neighbors(adjacency_graph, v) do
13:    if color[w]  $\neq$  0 then
14:      for each  $(x, \text{index\_wx}) \in$  indexed_neighbors(adjacency_graph, w) do
15:        if color[x]  $\neq$  0 and forbidden_colors[color[x]]  $\neq$  v then
16:          root_wx  $\leftarrow$  find_root(forest, index_wx)
17:          (p, q)  $\leftarrow$  first_visit_to_tree[root_wx]
18:          if p  $\neq$  v then
19:            first_visit_to_tree[root_wx]  $\leftarrow$  (v, w)
20:          else if q  $\neq$  w then
21:            forbidden_colors[color[x]]  $\leftarrow$  v
22:          end if
23:        end if
24:      end for
25:    end if
26:  end for
27:  color[v]  $\leftarrow$  min{i | forgiven_colors[i]  $\neq$  v}
28:  for each  $(w, \text{index\_vw}) \in$  indexed_neighbors(adjacency_graph, v) do
29:    if color[w]  $\neq$  0 then
30:      (p, q, index_pq)  $\leftarrow$  first_neighbor[color[w]]
31:      if p  $\neq$  v then
32:        first_neighbor[color[w]]  $\leftarrow$  (v, w, index_vw)
33:      else
34:        root_vw  $\leftarrow$  find_root(forest, index_vw)
35:        root_pq  $\leftarrow$  find_root(forest, index_pq)
36:        root_union(forest, root_vw, root_pq)
37:      end if
38:    end if
39:  end for
40:  for each  $(w, \text{index\_vw}) \in$  indexed_neighbors(adjacency_graph, v) do
41:    if color[x] == color[v] then
42:      root_vw  $\leftarrow$  find_root(forest, index_vw)
43:      root_wx  $\leftarrow$  find_root(forest, index_wx)
44:      if root_vw  $\neq$  root_wx then
45:        root_union(forest, root_vw, root_wx)
46:      end if
47:    end if
48:  end for
49: end for

```

Algorithm C.5: Procedure acyclic_coloring.

```

Input:
    • adjacency_graph, nv, ne, nt, forest
Output:
    • nvmax, tree_edge_indices, tree_vertices, tree_neighbor_indices, tree_neighbors
1: tree_vertices[1,...,ne+nt] ← 0
2: tree_neighbor_indices[1,...,ne+nt+1] ← 0
3: tree_neighbors[1,...,2*ne] ← 0
4: tree_edge_indices[1,...,nt+1] ← 0
5: root_to_tree[1,...,ne] ← 0
6: visited_trees[1,...,nt] ← 0
7: vertex_position[1,...,nt] ← 0
8: neighbor_position[1,...,nt] ← 0
9: nr ← 0
10: for index_edge ← 1 to ne do
11:     root ← find_root(forest, index_edge)
12:     if root_to_tree[root] == 0 then
13:         nr += 1
14:         root_to_tree[root] ← nr
15:     end if
16:     index_tree ← root_to_tree[root]
17:     tree_edge_indices[index_tree + 1] += 1
18: end for
19: nvmax ← maximum(tree_edge_indices) + 1
20: vertex_position[1] ← 0
21: neighbor_position[1] ← 0
22: for k ← 2 to nt do
23:     vertex_position[k] ← vertex_position[k-1] + tree_edge_indices[k] + 1
24:     neighbor_position[k] ← neighbor_position[k-1] + 2 * tree_edge_indices[k]
25: end for
26: for j ← 1 to nv do
27:     for each (i, index_ij) ∈ indexed_neighbors(adjacency_graph, j) do
28:         if i ≠ j then
29:             root ← find_root(forest, index_ij)
30:             index_tree ← root_to_tree[root]
31:             vertex_index ← vertex_position[index_tree]
32:             if visited_trees[index_tree] ≠ j then
33:                 visited_trees[index_tree] ← j
34:                 vertex_position[index_tree] += 1
35:                 vertex_index += 1
36:                 tree_vertices[vertex_index] ← j
37:             end if
38:             neighbor_position[index_tree] += 1
39:             neighbor_index ← neighbor_position[index_tree]
40:             tree_neighbors[neighbor_index] ← i
41:             tree_neighbor_indices[vertex_index + 1] += 1
42:         end if
43:     end for
44: end for
45: tree_edge_indices[1] ← 1
46: tree_neighbor_indices[1] ← 1
47: for k = 2 to nt+1 do
48:     tree_edge_indices[k] ← tree_edge_indices[k] + tree_edge_indices[k-1]
49:     tree_neighbor_indices[k] ← tree_neighbor_indices[k] + tree_neighbor_indices[k-1]
50: end for

```

Algorithm C.6: Procedure to recover the structure of the trees from forest.

Input:

- `nvmax` is the number of vertices in the largest tree of the forest.
- `tree_edge_indices` specifies the starting and ending indices of edges for each tree.
- `tree_vertices` contains the list of vertices, grouped by tree.
- `tree_neighbor_indices` provides the positions of the first and last neighbors for each vertex in `tree_vertices`, within the tree to which the vertex belongs.
- `tree_neighbors` is a packed representation of the neighbors of each vertex in `tree_vertices`.

Output:

- `reverse_bfs_orders` is the edge ordering used for decompression, grouped by tree.
- `is_star` is a boolean vector indicating whether each tree is a star.

```

1: reverse_bfs_orders[1,...,ne] ← (0,0)
2: degrees[1,...,nv] ← 0
3: reverse_mapping[1,...,nv] ← 0
4: queue[1,...,nvmax] ← 0
5: is_star[1,...,nt] ← false
6: num_edges_treated ← 0
7: for k = 1 to nt do
8:   queue_start ← 1
9:   queue_end ← 0
10:  first_vertex ← tree_edge_indices[k] + k - 1
11:  last_vertex ← tree_edge_indices[k + 1] + k - 1
12:  for index_vertex in first_vertex:last_vertex do
13:    vertex ← tree_vertices[index_vertex]
14:    index_first_neighbor = tree_neighbor_indices[index_vertex]
15:    degree = tree_neighbor_indices[index_vertex+1] - index_first_neighbor
16:    degrees[vertex] ← degree
17:    reverse_mapping[vertex] ← index_vertex
18:    if degree == 1 then
19:      queue_end += 1
20:      queue[queue_end] ← vertex
21:    end if
22:  end for
23:  nv_tree ← tree_edge_indices[k + 1] - tree_edge_indices[k] + 1
24:  is_star[k] ← queue_end ≥ nv_tree - 1
25:  while queue_start ≤ queue_end do
26:    leaf ← queue[queue_start]
27:    queue_start += 1
28:    degrees[leaf] ← 0
29:    index_leaf ← reverse_mapping[leaf]
30:    first_neighbor ← tree_neighbor_indices[index_leaf]
31:    last_neighbor ← tree_neighbor_indices[index_leaf + 1] - 1
32:    for index_neighbor in first_neighbor:last_neighbor do
33:      neighbor ← tree_neighbors[index_neighbor]
34:      if degrees[neighbor] ≠ 0 then
35:        num_edges_treated += 1
36:        reverse_bfs_orders[num_edges_treated] ← (leaf, neighbor)
37:        degrees[neighbor] -= 1
38:        if degrees[neighbor] == 1 then
39:          queue_end += 1
40:          queue[queue_end] ← neighbor
41:        end if
42:      end if
43:    end for
44:  end while
45: end for

```

Algorithm C.7: Procedure to compute the reverse BFS order of the trees.

Input:

- **buckets**: a vector of stacks, one per degree
- **v**: a vertex to be moved up one degree

```

1:  $d \leftarrow$  current dynamic degree of  $v$ 
2:  $p \leftarrow$  position of  $v$  inside  $\text{buckets}[d]$ 
3:  $w \leftarrow \text{buckets}[d][\text{end}]$ 
4:  $\text{buckets}[d][p] \leftarrow w$ 
5:  $\text{buckets}[d][\text{end}] \leftarrow v$ 
6:  $\text{pop\_last}(\text{buckets}[d])$ 
7:  $\text{append\_last}(\text{buckets}[d+1], v)$ 
8: record new positions of  $v$  and  $w$ 

```

Algorithm C.8: Stack-based degree bucket update, following ColPack.

Input:

- **bucketvec**: a vector of integers, one per vertex
- **bucketlims**: a vector of integer pairs, one per degree
- **v**: a vertex to be moved up one degree

```

1:  $d \leftarrow$  current dynamic degree of  $v$ 
2:  $p \leftarrow$  position of  $v$  inside  $\text{buckets}[d]$ 
3:  $(a, b) \leftarrow \text{bucketlims}[d]$ 
4:  $(a_{\text{up}}, b_{\text{up}}) \leftarrow \text{bucketlims}[d+1]$ 
5:  $w \leftarrow \text{buckets}[d][\text{end}]$ 
6:  $\text{bucketvec}[a+p] \leftarrow w$ 
7:  $\text{bucketvec}[a_{\text{up}}-1] \leftarrow v$ 
8:  $\text{bucketlims}[d] \leftarrow (a, b-1)$ 
9:  $\text{bucketlims}[d+1] \leftarrow (a_{\text{up}}-1, b_{\text{up}})$ 
10: record new positions of  $v$  and  $w$ 

```

Algorithm C.9: Vector-based degree bucket update, introduced in SMC.